

Exchanges

No. 32 (Vol 10, No.1)

January 2005

Seasonal Predictability

Latest CLIVAR News

<http://www.clivar.org/recent/>

See the **CLIVAR** Calendar

<http://www.clivar.org/calendar/index.htm>

This issue has been sponsored by the China Meteorological Administration through the Chinese Academy of Meteorological Sciences



CLIVAR is an international research programme dealing with climate variability and predictability on time-scales from months to centuries.



CLIVAR is a component of the World Climate Research Programme (WCRP). WCRP is sponsored by the World Meteorological Organization, the International Council for Science and the Intergovernmental Oceanographic Commission of UNESCO.

From Chen et al Page 21: Seasonal Forecast of Antarctica Sea Ice

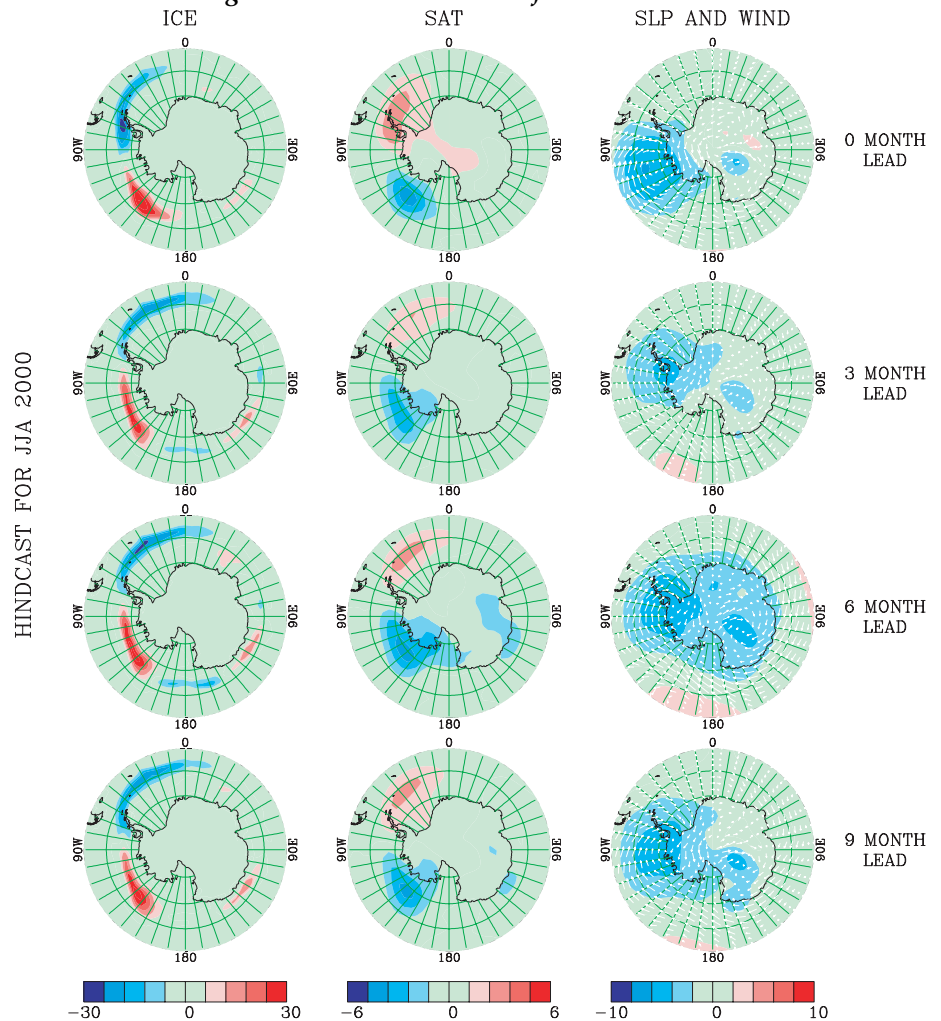


Figure 1. Model hindcasts at different lead times for anomalous sea ice concentration and associated atmospheric conditions in JJA, 2000. The top row (0-month lead) may be regarded as the target to predict.

Call for Contributions

Due to the oversubscription of articles for Seasonal Predictability (no. 32, January 2005), the following issue of Exchanges (no.33, April 2005) will continue this theme.

The Asian Monsoon edition will now be no. 34 (July 2005) with a submission deadline of 30th April 2005 and not 31st January as advertised on the front cover of issue 31.

Editorial

The last year has been a busy one for CLIVAR, not least because of the highly successful CLIVAR Conference and the review of CLIVAR undertaken by the Scientific Steering Group immediately following. In addition, CLIVAR Panels and Working Groups have been continuing to develop various aspects of the CLIVAR programme. Seasonal Prediction, to which much of this edition of Exchanges is devoted, is an important activity not only for CLIVAR but also for WCRP as a whole. Indeed the Task Force on Seasonal Prediction (TFSP) was the first such activity to be set up under WCRP's Coordinated Observation and Prediction of the Earth System (COPEs) strategy. The TFSP is chaired by Ben Kirtman, who also co-chairs CLIVAR's Working Group on Seasonal to Interannual Prediction (WGSIP) with Tim Stockdale. It has proposed a major pan-WCRP "Total Climate System Prediction Experiment" to test the hypothesis that *"there is currently untapped coupled predictability due to interaction and memory associated with all the elements of the climate system (atmosphere-ocean-land-ice)"*. This proposal was welcomed and endorsed by the Joint Scientific Committee (JSC) for WCRP who asked the TFSP to continue to develop and refine its proposal for discussion at the next session of the JSC which takes place in Guayaquil, Ecuador in March.

Progress with WGSIP activities was reviewed and further developed when WGSIP met at the Met Office in Exeter, UK from 14-16 October 2004. The group agreed to develop its "standards project" aimed at open, ongoing protocols for model comparisons through an El Niño pilot project which is being developed and will be announced following the group's next meeting. Following the request from CLIVAR's SSG to strengthen the links between CLIVAR's global and regional activities (see the article by Tim Palmer and Tony Busalacchi below), the group also agreed on a number of initiatives to develop the interactions with CLIVAR's Pacific, American Monsoon (VAMOS) and African (VACS) Panels, in particular both in terms of joint experiments (Pacific) and model data provision (VAMOS & VACS).

Other interactions with WCRP's GEWEX, the Working Group on Numerical Experimentation, the International Climate of the 20th Century Project (a CLIVAR-sponsored activity) and to the Applications community are also being pursued. International participation in WGSIP's Seasonal Model Intercomparison Experiment continues to be strongly encouraged whilst an emerging area of activity is that of the potential for a WGSIP contribution on Observation System Simulation Experiments relevant to seasonal prediction.

Following the WGSIP meeting itself, a WGSIP Workshop on Ensemble Methods was held from 18-21 October 2004. The wide interest and activity in ensemble approaches and methods was clearly reflected in the enthusiasm expressed for attending the Workshop (over 160 registrants) and in the scientific level of the presentations made (10 invited and approximately 50 each oral and poster presentations). CLIVAR is grateful both to George Boer for organising the Workshop and to the Met Office for acting as hosts. The electronic Proceedings of the Workshop can be viewed at: <http://cccma.seos.uvic.ca/ensemble/>

CLIVAR's Panels' and Working Groups are the engine by which CLIVAR progresses. Each of these is made up of some dozen internationally respected scientists who serve, under the leadership of their respective chair or co-chairs, to develop the implementation of CLIVAR in their areas of science. Information on the CLIVAR Panels and Working Groups can be found on the CLIVAR Home Pages (www.clivar.org). Membership is usually on a 4-year rotational basis and CLIVAR is always interested in suggestions for new members. If you are interested in becoming a member of one of CLIVAR's Panels or Working Groups we will be pleased to hear from you. Please send your self-nomination to the ICPO at icpo@soc.soton.ac.uk together with a short paragraph of background and we will add names to a register of interest.

Howard Cattle

CLIVAR – The Regional/Global Dichotomy

A Busalacchi and T.N.Palmer (Co-chairs, International CLIVAR Scientific Steering Group)

CLIVAR's mission "To observe simulate and predict Earth's climate system, with a focus on ocean-atmosphere interactions, enabling better understanding of climate variability predictability and change, to the benefit of society and the environment in which we live" is wide-ranging! In order to realise its mission, CLIVAR has created a number of panels, dividing the project as a whole into a set of manageable parts. Many of these panels (AAMP, VACS, VAMOS and the Ocean Basin

Panels) have regional foci, whilst the perspective of others (WGSIP, WGCM, WGOMD and GSOP) is primarily global. This regional/global dichotomy is an essential aspect of CLIVAR. On the one hand observations are made locally, and the value of climate forecasts is determined by their influence on the lives of individuals. On the other hand, the tools we use to assimilate these observations and to make these climate predictions are increasingly global in domain. As discussed at the last

CLIVAR SSG meeting, one of the challenges for CLIVAR is to develop a strategy for development which draws explicitly on this dichotomy.

One of the major achievements of the climate community in recent years has been the production of global analysis and climate re-forecast datasets. The relevant datasets can be freely downloaded on the web. We are all aware of the reanalysis datasets (e.g. ERA40 (www.ecmwf.int/research/era40), and NCEP (www.cdc.noaa.gov/ncep_reanalysis). In addition, CLIVAR has been particularly active in the development of multi-model climate hindcast datasets: SMIP (www-pcmdi.llnl.gov/smip) and DEMETER (www.ecmwf.int/research/demeter) for seasonal prediction and CMIP (www-pcmdi.llnl.gov/cmip) for climate change prediction. (Indeed, the development of such multi-model ensemble datasets was explicitly recognised in the recent CLIVAR review process, as one of the success stories of CLIVAR.) At the present time, a new multi-model dataset is being produced for the IPCC AR4 (www.ipcc.ch) - see CLIVAR Exchanges No 30 for details. Analyses of these integrations are being discussed at a workshop convened by US CLIVAR at IPRC Honolulu (1-4 March 2005). Finally, in the coming year or so, global multi-model seasonal, decadal and centennial climate prediction datasets will become available as part of the EU ENSEMBLES project (www.ensembles-eu.org).

The diagnostic analysis of these global datasets at the regional level, presents an opportunity to develop more strongly the links between CLIVAR science on the global

scale and at the regional level. The analysis could, for example, be addressed at quantifying and understanding regional predictability of seasonal climate variability or at the systematic error characteristics of the current generation of climate models to simulate regional climate variations on different timescales.

In the case of climate change, such analyses will get to the heart of what has often been seen as the essence of the unique CLIVAR perspective on climate change: analysis of how anthropogenic forcing can influence the natural patterns of climate variability. For example, to what extent can anthropogenic climate-change forcing on the Asian monsoon be understood in terms of changes to the frequency of occurrence of the main patterns of intraseasonal and interannual variability of monsoon activity? Similarly, how is the decadal mode associated with Sahel drought influenced by anthropogenic forcing? To what extent do the models to be used in IPCC AR4, satisfactorily describe the coupled dynamics of ENSO? How is the frequency of ENSO influenced by anthropogenic forcing.

We ask CLIVAR scientists to consider the opportunities presented by these new datasets, and to engage with the relevant CLIVAR panels in the analysis of these datasets. Through such endeavours we can advance CLIVAR science on both the global scale and the regional level.

We invite your comments on these matters. Please send them to the International CLIVAR Project Office (icpo@soc.soton.ac.uk)

The CLIVAR and Carbon Hydrographic Data Office at the UCSD Scripps Institution of Oceanography

The fundamental purpose of the CLIVAR and Carbon Hydrographic Data Office (CCHDO; formerly and concurrently the WOCE Hydrographic Program Office or WHPO) is to see that WOCE Hydrographic Program (WHP) data, CLIVAR repeat hydrography data, global ocean carbon hydrographic data, and other similar CTD/hydrographic data and their associated documentation are prepared and made available for both immediate use and a long service life.

During WOCE the WHPO was an intermediary between investigators carrying out WOCE CTD/hydrographic field work, investigators making use of WHP ocean profile data, and the national and international archive centers. At the WHPO, the CTD, hydrographic, and so-called tracer data used in ocean circulation studies were brought together, verified, assembled with relevant documentation, and carefully prepared for dissemination and archive. In addition the WHPO served as a proactive force in the hydrographic data community, working to promote appropriate methodology, applicable community standards, communications, and data compatibility.

The need for WHPO-like services has not abated with the end of WOCE. For example currently CLIVAR and global ocean carbon programs generate significant volumes of WHP-like data, the emphasis being establishing the temporal variability in key ocean regions over annual, decadal, and century time scales. Simply put, to be of use to long-term studies these data must be carefully collected and unambiguously documented and preserved to be useful to current and future oceanographic research.

The most important functions connected with this are

- (1) locating data and arranging for data and documentation transfer to a data office,
- (2) checking all data and headers for errors and correcting those errors,
- (3) merging bottle data parameters from disparate sources,
- (4) moving the data into tight agreement with well-specified community data formats,
- (5) bringing together, organizing, and preserving the information about the data necessary to understand and use them for generations, and

(6) providing for widespread distribution of the data and archive of the data.

Despite the cost of supporting a data office, it is efficient in the short run and essential in the long run to carry out these functions at a single, well organized, experienced facility.

Data acquisition and assembly: The data office acquires data and documentation in activist mode, i.e. soliciting individual investigators and data providers (not only Chief Scientists) by mail, email, fax, telephone, inquiries and reminders to investigators, institutions and national committees

Data are accepted in any readable format but preference is given to the formats supported by the office. Preliminary data and documentation are accepted, in which case the data office works with investigators to arrive at a mutually-acceptable timeline for completion. The CCHDO maintains a data catalogue and tracks and documents data modifications as well as ancillary information such as measurement and submittal dates, proprietary status, and so forth for each data subset.

The CCHDO is a data assembly center. For example, bottle data parameters are typically received from several investigators. To the uninitiated it may seem simple to bring these together into a single bottle data file - and maybe it should be simple - but nearly every imaginable problem seems to arise.

Quality control: The data office uses a hierarchy of data quality control procedures to ensure the highest possible standard of data accuracy and utility. The process includes providing example data and documentation files, validating data for content and format, and preparation of a corrected-for-readability version of the data file.

More often than not, data are received in less than desirable condition. Problems include conflicting header and sample information, missing values, incorrect values, wrong units, lack of information about the files themselves, version control problems, data in individual station files or continuous strings, data not in ASCII, etc.

Sometimes a data originator is unreachable or uncooperative. With this in mind it is no surprise that repairing data problems is truly a massive undertaking. Though the office has worked hard to streamline this, for some cruises there is a great deal of work required. But it can be said that once files go on line at the CCHDO, with very few (if any) exceptions, if one can read one WHP-Exchange data file, one can read any other WHP-Exchange data file.

During WOCE there was a subsequent data quality control process involving intensive Data Quality Examination ('DQE') carried out by community data experts. The CCHDO continues cleaning the data files, parameter by parameter, for errors and improved adherence to specified community formats, but has discontinued external DQE.

Data access: Access to data held by the office is provided primarily by on-line service and secondarily by data CD-ROMs, which are essentially copies of the on-line site.

Data version control and data originator citation: The office has long kept track of and made available data history and data originator information for every data set. But the CCHDO now goes beyond this (for most new cruises) by embedding key file version, investigator, and citation information in the 'comment' lines in new WHP-Exchange data files for the CLIVAR and global ocean carbon programs. This lists all previous CCHDO versions of that file, all data originators, plus the American Geophysical Union requirements for citation of data.

Data archive: The office provides all publicly-available data and documentation to the archive at NODC/WDC-A.

Documentation: The office prepares as complete a pdf documentation set as feasible for each cruise, including cruise reports, final reports and amendments received from the Chief Scientist and other participating investigators, and summaries of in-office data notes and file information.

Investigator support: The office maintains on-line information about each cruise, including (among much else) investigator contact information. Maps and search capabilities guide investigators to data of interest. Additionally the office maintains an on-line library of electronic documentation of cruise reports and other documents.

In summary, the CLIVAR repeat hydrography, global ocean carbon, and similar hydrographic data will be created by >100 data originators, sometimes 5-8 contributing to what becomes one bottle data file. One way or another all data *users* must cope with the temporal-, content-, and format-related file diversity these different originators produce. It the enormous advantage of merging diverse data and especially bringing all data sets to a common content and readability standard that remains the strongest argument for having a service such as now provided by the CCHDO, with a strong additional advantage that the documentation associated with the data are collected, reorganized to a common standard (where possible), and preserved with the data.

Preliminary study of the East African short rains predictability at the monthly and grid-point scales (1968–1998)

N. Philippon, P. Camberlin, CRC, Dijon, France
Corresponding email: nphilipp@u-bourgogne.fr

1. Introduction:

Forecasting rainfall amounts in tropical regions is a challenge because of the strong impact rainfall variability has on major socio-economic activities (agriculture, energy supply...). Since the 1980s, the scientific community has performed numerous rainfall predictability studies and currently runs, along with GCMs, operational statistical forecasting models. However the scales considered in these studies and statistical models (regional and seasonal ones) are still too large to be of valuable benefit for local communities.

The October-December East African short rains compared for instance to the July-September Sahelian rainy season, show a relatively high degree of predictability: statistical forecasting models usually reproduce about 50% of the total variance of this rainy season using global sea surface temperatures (SST) fields of the preceding months (Mutai et al 1998, Thiaw et al 1999). More recently, based on September oceanic-atmospheric regional signals, Philippon et al (2002) increased the explained variance of the short rains up to 64%. The high predictability of the short rains at "large" scale, coupled (and linked) to their strong spatial coherency, make them an interesting candidate to explore rainfall predictability at finer scales.

This note aims at presenting the preliminary results of an attempt to evaluate the short rains predictability at the monthly and the grid-point scales. After recalling the characteristics of the statistical model developed by Philippon et al (2002) for the seasonal and regional scales, the results obtained by a direct downscaling of this model are presented. The next section proposes an approach to evaluate the predictability of the small scale residual variability.

2. Direct downscaling from the seasonal rainfall index to the monthly fields

2.a Characteristics of the seasonal and regional statistical model:

Figure 1 locates the October-December rainfall index "KURI" and the 3 September oceanic-atmospheric indexes "MDI", "PCO" and "V200" entered respectively as "predictand" and "predictors" in a Multiple Linear Regression (MLR) model by Philippon et al (2002, details regarding the predictors can be found here). Run in a 1-year cross-validation mode over the period 1968-1997, this statistical model reproduces 64% of KURI variability ($r=0.81$).

2.b Model performance at the monthly and grid-point scales:

To evaluate the short rains predictability at finer scales, the predictand has been redefined as the rainfall fields

at a $0.5^\circ \times 0.5^\circ$ resolution over the region $10^\circ\text{S}-6^\circ\text{N}/30-42^\circ\text{N}$ for each month of the rainy season (these fields have been computed from the CRC monthly raingauge database). Statistical MLR models using the above three predictors are computed for each grid-point and each month.

Figure 2 (page 7) presents the resulting correlation maps between the observed and modelled October to December rainfall fields. What emerges is that the model defined for the seasonal and regional scale, performs quite well at finer scales. In October and November particularly, some grid-points have up to 50% of their variance reproduced. However and logically, these grid-points are mainly enclosed in the "KURI" region; the variability over the southern areas and parts of the Kenya Highlands is generally not adequately predicted.

3. Predictability of the fine scale residual variance of October:

3.1 Methodology:

The approach developed to evaluate October rainfall predictability at small scales is composed of two steps. In the first step, a rainfall residual field is computed: it consists in the difference between the observed field and that obtained from the MLR models (Fig2.a). In a second step, the residual rainfall field is entered in a Canonical Correlation Analysis (CCA) jointly with the synchronous 700hPa wind field over $10^\circ\text{N}-15^\circ\text{S}/25-50^\circ\text{E}$ (extracted from the NCEP/NCAR reanalyses, Kalnay et al, 1996).

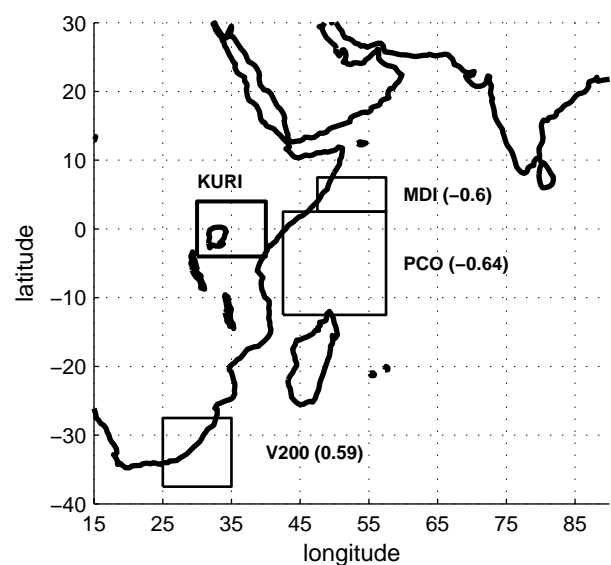


Figure 1: location of KURI and its 3 September predictors. Bracketed : their partial correlation with KURI.

The choice of the 700hPa level and of a regional domain is motivated by the assumption that rainfall anomalies at small scales are first driven by local mid-tropospheric dynamical conditions. Both the rainfall and wind fields have been initially submitted to Principal Component Analyses. The first five PCA rainfall modes and the first eleven wind modes (explaining 65% and 90% of the total variance, respectively) have been retained as input in the CCA.

3.2 Preliminary results for October:

Only the second CCA mode is retained in this study. It mainly associates an east-west rainfall dipole (Fig.3a) to zonal wind anomalies above the region (Fig.3b). Wet (dry) conditions in the west (east) prevail when easterlies are weakened. The expansion coefficients for wind and rainfall (Fig.3c) are correlated at 0.84.

In order to understand the mechanisms responsible for the wind anomalies and detect potential predictive signals for rainfall, the wind expansion coefficient has been correlated to the September and October sea-surface temperature (obtained from the GISST2.3b database, Rayner et al, 1996) as well as to the air temperature and wind fields from 925 to 200hPa, independently from PCO, V200 and MDI. Only the correlation maps depicting SST and 300hPa atmospheric fields are provided on figures 4 (page 8) and 5 (page 15).

Two distinctive, large-scale signals, observed as soon as September, appear. The first one, at the surface, concerns SST anomalies in the south tropical Atlantic (Fig 4.a, b). The role of this basin was supposed to be already taken into account through the index 'V200'. However, V200 does not fully describe the basin variability; for example, a correlation of 0.36 (0.19) is found between V200 and a September (October) south Atlantic SST index in the region [10-20°S, 10-20°W]. An anomalous warming (cooling) of the basin is associated with enhanced (weakened) easterly winds, and higher (lower) rainfall in the eastern, windward (western, leeward) parts of East Africa (Camberlin and Wairoto, 1997; Philippon et al, 2002).

The second signal mainly stands in the upper troposphere (Fig 5.a, b) as two broad bands of temperature anomalies over the subtropics, symmetrical about the equator. This signal has been shown by Liu and Yanai (2001) to be related to the Indian monsoon: a warming of the Eurasian upper troposphere indicates an active monsoon, the coupling being the strongest in autumn (September-October). Preliminary correlation analyses between a September index of temperature at 300hPa over Eurasia and October wind fields at 300, 700 and 925hPa indicate that a delayed weakening of the southern Hadley cell (stronger and northward TEJ in the upper troposphere and south-westerly flow at the surface) is accompanied by a slowing down of easterly winds from 925 to 700hPa over East Africa.

4. Conclusion:

The direct downscaling of a robust MLR model established for a seasonal and regional rainfall index to predict rainfall variability at monthly and grid-point scales performs relatively well for October and November with up to 50% of the rainfall variance explained at some points. The residual rainfall variability in October has been coupled to the regional mid-tropospheric October wind field trough CCA. The second mode is characterized by an east-west dipole in the rainfall field associated with anomalies in the zonal wind. Preliminary correlation analyses between the wind expansion coefficient and September SST and atmospheric dynamics point out anomalies in the south tropical Atlantic and the upper troposphere, the latter related to the Indian monsoon. Both act on the intensity of the equatorial easterly (westerly) winds east of East Africa (over the Congo basin). It is noticeable that whereas rainfall anomalies are considered at smaller scales, the predictive signals highlighted still involve large scale dynamics and teleconnections.

References:

- Camberlin, P. and J. Wairoto, 1997: Intraseasonal wind anomalies related to wet and dry spells during the 'long' and 'short' rainy seasons in Kenya, *Theor. Appl. Climatol.*, 58, 57-69.
- Kalnay, E. and co-authors, 1996: The NCEP-NCAR 40 year Reanalyses Project, *Bull. Amer. Meteor. Soc.*, 77, 437-471.
- Liu, X. and M. Yanai, 2001: Relationship between the Indian monsoon rainfall and the tropospheric temperature over the Eurasian continent, *Q.J.R. Meteorol. Soc.*, 127, 909-937.
- Mutai, C.C., N. Ward and A.W. Colman, 1998: Towards the prediction of the East African short rains based on sea-surface temperature-atmosphere coupling, *Int. J. Climatol.*, 18, 975-997.
- Philippon, N., P. Camberlin and N. Fauchereau, 2002: Empirical predictability study of October-December East African rainfall, *Q.J.R. Meteorol. Soc.*, 128, 2239-2256.
- Rayner, N.A., E.B. Horton, D.E. Parker, C.K. Folland and R.B. Hackett, 1996: Version 2.2 of the global sea-ice and sea surface temperature data set, 1903-1994, *Hadley Centre, Technical Note*, 74, 21p.
- Thiaw, W., A.G. Barnston and V. Kumar, 1999: Predictions of African rainfall on the seasonal timescale, *J. Geophys. Res.*, 104, 31589-31597.

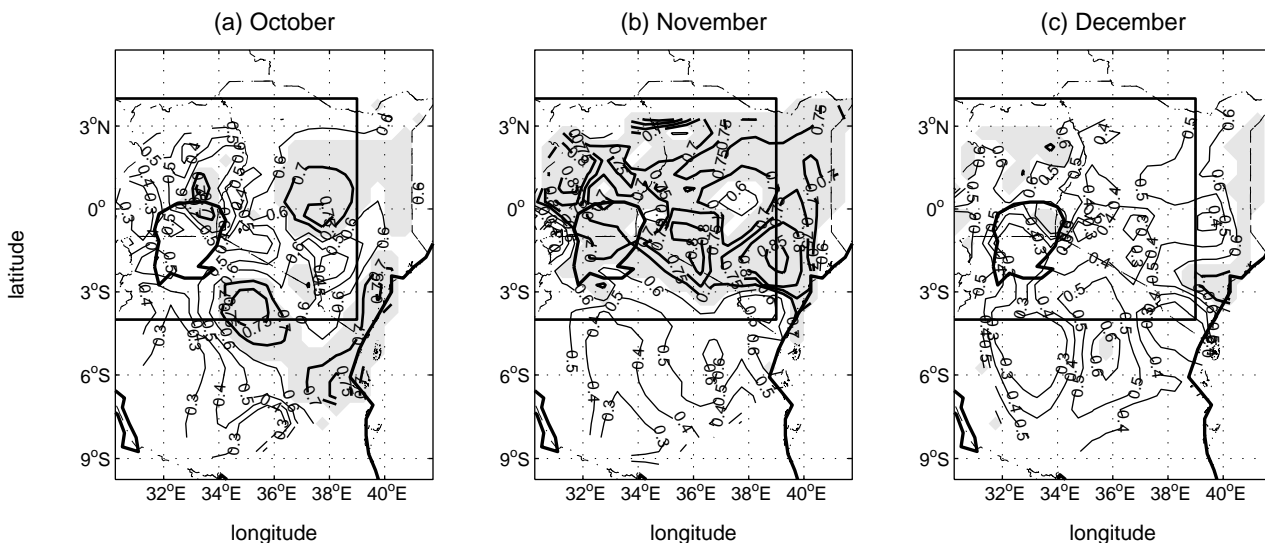


Figure 2: correlation between observed and modelled (a) October, (b) November and (c) December rainfall fields using a Multiple Linear Model fed with 'PCO', 'V200' and 'MDI', the 3 September predictors of KURI. Shading indicates grid-points having more than 40% of their variance reproduced. The box delineates Kuri domain.

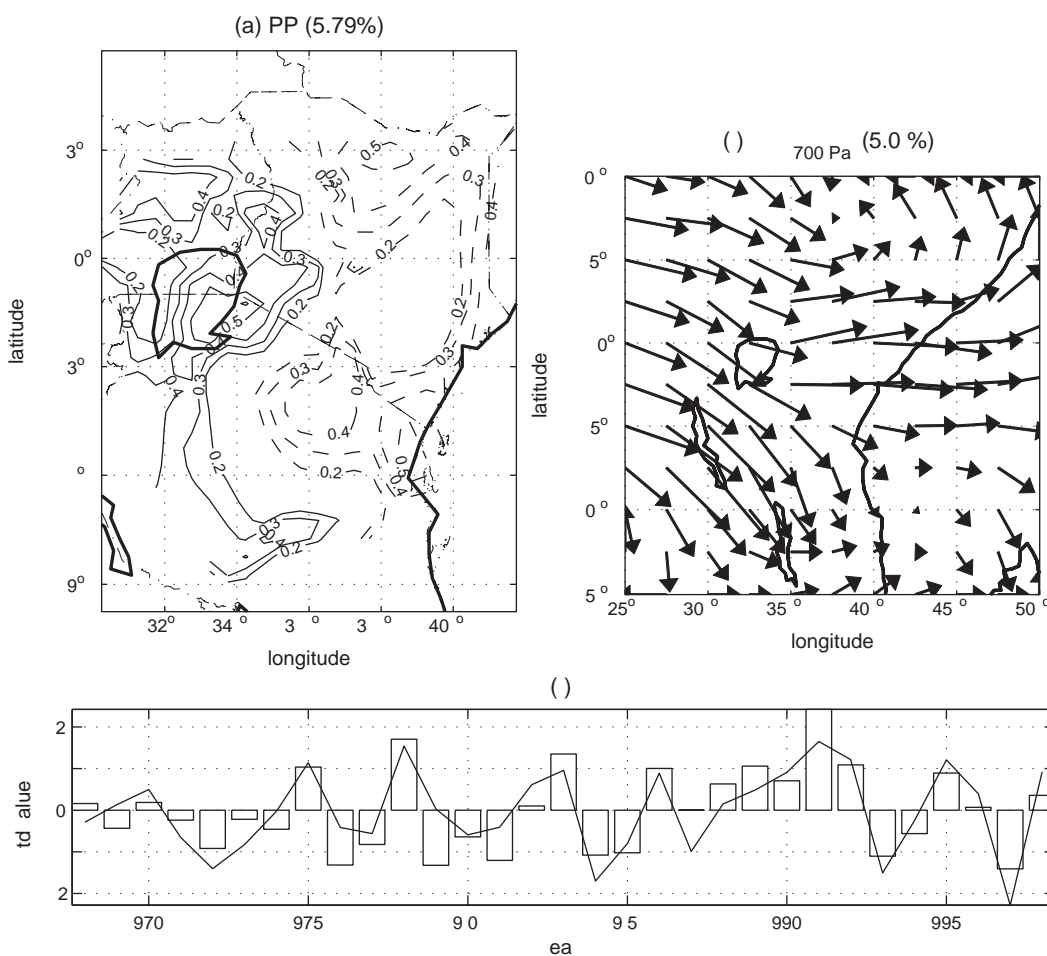


Figure 3: (a) heterogeneous correlation pattern of rainfall, (b) homogeneous correlation pattern of the 700 hPa wind field and (c) their respective expansion coefficients (bars for rainfall and line for wind) for the second CCA mode in October.

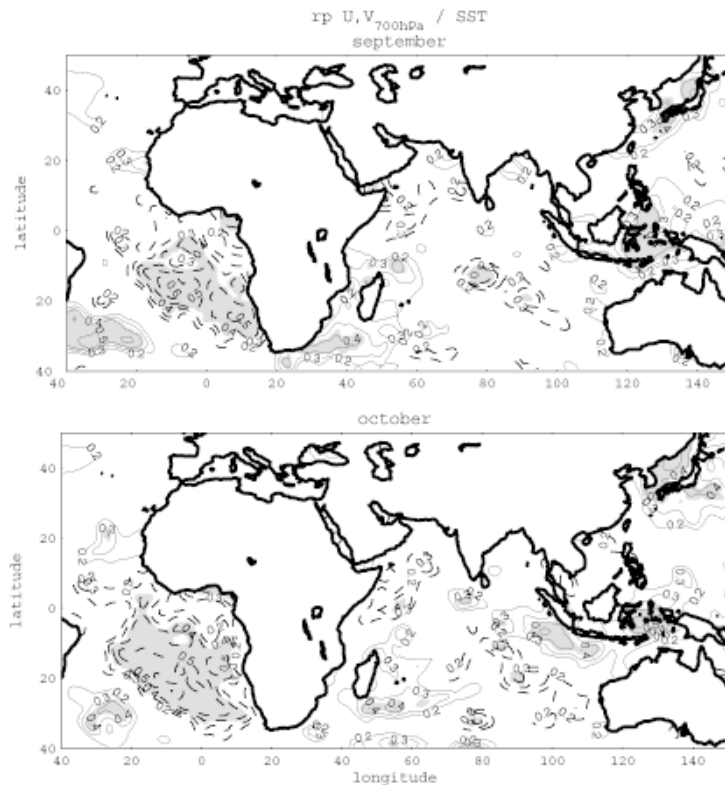


Figure 4: correlation maps between the October wind expansion coefficient and (a) September, (b) October SST field independently from 'PCO', 'V200' and 'MDI'. Shading indicates grid-points significantly correlated at the 95% level.

Multi-Model Ensembling: Refining and Combining

Lisa Goddard, Simon J. Mason and Andrew W. Robertson

International Research Institute for Climate Research, The Earth Institute of Columbia University, Palisades, New York, USA

Corresponding author: goddard@iri.columbia.edu

1. Introduction

Dynamical models are increasingly the prediction tool of choice by seasonal forecast centers. They encapsulate the full physics of the atmosphere and thus are less prone to the limitations of empirical models, such as those due to finite observational records or climate stationarity. However, dynamical models or general circulation models (GCMs) have their limitations also, primarily associated with the parameterizations necessary to describe physical processes occurring on spatial and temporal scales smaller than are resolved by the GCMs.

As shown in Figure 1 (page 15), individual models each have regions where they do better or worse than the other models. By simply combining them all into 1 super-ensemble, deficiencies seen in individual models are reduced. However, by taking into account which models work where, and perhaps under what conditions, we can improve over the straightforward pooling of models. How much and in what ways more sophisticated multi-model combinations can improve over the baseline of pooling is the focus of this work, which is more an illustration and comparison of techniques than a quantitative examination of real-time forecast skill.

2. Data & Verification

The model data are taken from 3 atmospheric GCMs. The CCM3.6 (Kiehl et al., 1998) and the ECHAM4.5 (Roeckner et al., 1996) AGCMs are configured at T42L18. The NSIPP1 AGCM (Bacmeister et al., 2000) is a grid point model with a horizontal resolution of 2x2.5 degrees and 34 vertical levels; NSIPP1 data were interpolated to T42 for the multi-model ensembling.

All AGCM predictions(/simulations) are cast as probabilistic 3-category forecasts for 3-monthly seasonal values of mean temperature and total rainfall, where the prior probability of any 1 category is 1/3. Because seasonal forecasts are probabilistic, they will be assessed as such.

The observations for temperature and precipitation, against which the model combinations are validated, come from the Climate Research Unit of the University of East Anglia (New et al., 2000). The data are provided at 0.5x0.5 degree resolution, and were upscaled to T42 for use in the validation.

The Ranked Probability Skill Score (RPSS) is the probabilistic measure of skill is used to validate the

forecast system against the observations. The RPSS measures the squared error between the cumulative forecast and observed probabilities, then weights that score against a reference forecast of climatology. A RPSS of 100% implies that the observed category was always predicted with 100% probability. A RPSS of 0 implies that the prediction performs as well as if climatological probabilities were always issued. A RPSS less than 0 implies the prediction system performs worse than climatology. Another perspective on probabilistic performance of the prediction system is gained through reliability diagrams. The goal is to produce *reliable* forecasts with good resolution, as this is necessary for forecasts to be useful in applications. This means that when a given probability is assigned to an event or a category it occurs in the observations with that frequency. However, a forecast system should also display sharpness, or have good resolution, meaning that the forecast probabilities should be able to deviate from climatological probabilities.

3. Multi-Model PDF Treatment & Combination Techniques

Two approaches are considered here for treating the model probability distributions and also for combining the probability distributions from the individual models. In each case, there is a more simple and less simple approach.

Refining

In the simplest case, no refinement of the model PDFs occurs. The model probabilities are taken straight from the AGCMs. This approach will be referred to as "Raw Probabilities".

The more complex approach refines the model PDFs, calibrating each model individually, based on the ensemble mean. The frequencies with which the observed category was below-normal, near-normal, and above-normal are tabulated for those times when the model's ensemble mean indicated a specific category. This is done seasonally for each variable at each grid point. A perfect deterministic forecast system would result in a purely diagonal matrix of 1s; a perfectly random prediction system would yield values of approximately 1/3 in every box (assuming 3 *a priori* equiprobable categories). With this matrix of conditional frequencies, one can construct a PDF from 'expected frequency' based on the model ensemble mean from the current seasonal forecast at a given location. This approach will be referred to as "Corrected Probabilities".

Combining

The simple approach for the combination is to weight each model equally. This approach will be referred to as "Pooled Multi-Model (MM) Ensemble".

The more complex approach weights the models spatially and seasonally based on past model performance for the variable of interest. The Bayesian approach to multi-model combination of AGCMs (Rajagopalan et al., 2002;

Robertson et al., 2004) determines the relative weights, pointwise, of each AGCM with climatology as the prior. The weights are chosen to maximize the likelihood score of the posterior (i.e., combined) probabilities. The climatology forecast has 33.3% probabilities for each category always. The AGCM probabilities change in each case. The result is that if the models have little or no skill over a particular region, climatology receives more or all the weight, and the resulting forecast for that location is closer to climatology. If one or more models frequently predict the observed category with confidence, then the model(s) receive more or all the weight, and the forecast appears closer to the models' probabilities. This approach will be referred to as the "Bayesian MM Ensemble".

4. Results

In comparing the more and less simple approaches to multi-model (MM) combination, reliability diagrams are used for an overall comparison. An example of the relative differences in reliability is illustrated in Figure 2 (page 10) for precipitation. The individual models are all over-confident in their probabilities, as evidenced by their horizontal slope. Little difference exists in the frequency of observed outcomes for either category shown whether the models indicate that the category is 20% likely or 80% likely. As shown in Figure 1, simple pooling of the AGCM ensembles leads to greater reliability – a more positive slope in the reliability curve.

For both temperature and precipitation, either correcting the PDF before combination, or using the Bayesian approach with the raw probabilities dramatically improves over the pooling of the raw AGCM probabilities (which is itself an improvement over the individual AGCMs). The corrected probabilities are almost perfectly reliable across the range of probabilities issued, which indicates excellent recalibration of the PDF. For the corrected probabilities, the additional improvement of the Bayesian MM combination does not provide much additional improvement to the reliability. The one potential shortcoming of the corrected probabilities is that the tails of the distribution are not represented; the forecasts are less sharp. This implies that the forecasts based on the corrected probabilities will be more conservative than those from the Bayesian approach with the raw PDFs. Note that climatology would be an almost perfectly reliable forecast, but there is no sharpness. Effectively the forecast contains no information. There is a need to balance reliability with forecast sharpness, or difference from climatological probabilities.

The apparent improvements in overall reliability also impact the local probabilistic skill (not shown). As the models perform better for temperature, the relative improvements from sophisticated treatment of the model PDFs and MM combination are less obvious than they are for precipitation. In general, for temperature, most of the improvements are seen to bring negative RPSS regions closer to 0; although there are a handful of regions

for which positive skill increases in the more sophisticated treatment relative to the baseline of pooled raw AGCM ensembles. For the precipitation, not only are negative values neutralized, but many coherent areas of positive skill in the baseline (raw pooled MM) improve, such as over western Africa, northern South America, and even Indonesia.

5. Conclusions

This study provides a preliminary investigation into possible methods for refining the PDFs of ensembles from dynamical models and combining them into a multi-model forecast. The baseline against which more sophisticated techniques were compared consists of straight pooling of the raw ensemble probabilities from the individual models.

Several conclusions emerge:

- AGCMs are over-confident in their probability distributions, and dynamical predictions benefit in skill and reliability from combining several models together.
- Further improved reliability of seasonal climate forecasts can be achieved by recalibrating the probability distributions either by directly "correcting" PDFs of the models or by weighting the models according historical probabilistic performance as in the Bayesian MM ensemble.

- For the techniques applied in this preliminary study, more sharpness is obtained from the Bayesian MM approach than from the corrected PDF approach.

References:

- Bacmeister, J., P.J. Pegion, S.D. Schubert, and M.J. Suarez, 2000: Atlas of Seasonal Means Simulated by the NSIPP 1 Atmospheric GCM. NASA/TM-2000-104505, Vol. 17, 190pp.
- Kiehl, J.T., J.J. Hack, G.B. Bonan, B.A. Boville, D.L. Williamson, and P.J. Rasch, 1998: The National Center for Atmospheric Research Community Climate Model, *J. Climate*, 11, 1131-1149.
- New, M., M. Hulme, and P.D. Jones, 2000: Representing twentieth-century space-time climate variability. Part II: Development of a 1901-96 monthly grid of terrestrial surface climate. *J. Climate*, 13, 2217-2238.
- Rajagopalan, B., U. Lall, and S.E. Zebiak, 2002: Categorical climate forecasts through a regularization and optimal combination of multiple GCM ensembles. *Mon. Wea. Rev.*, 130, 1792-1811.
- Robertson, A.W., U. Lall, S. E. Zebiak, and L. Goddard, 2004: Improved combination of atmospheric GCM ensembles for seasonal prediction. *Mon. Wea. Rev.*, in press.
- Roeckner, E., and co-authors, 1996: Simulation of the present-day climate with the ECHAM model: Impact of model physics and resolution. Report No. 93, Max-Planck-Institut für Meteorologie, Hamburg, Germany, 171pp

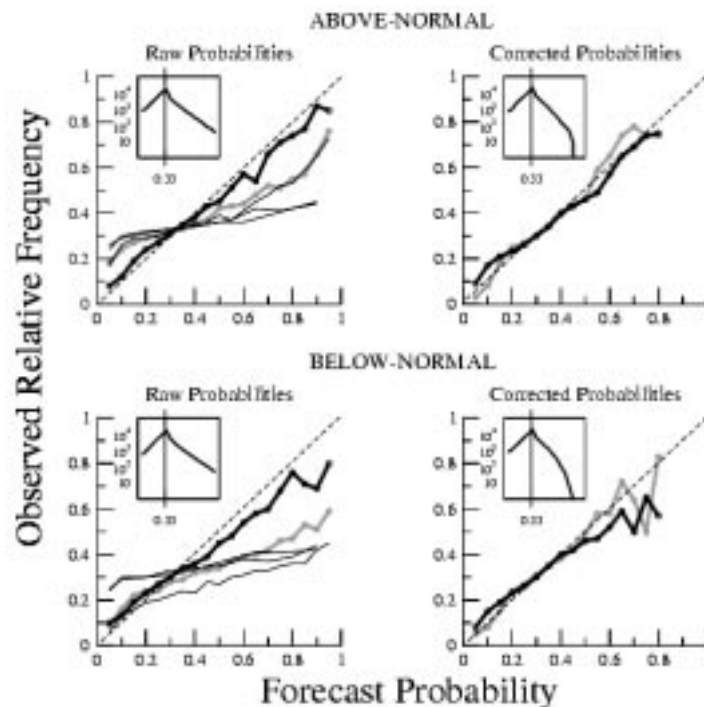


Figure 2. Reliability diagrams for JAS precipitation forecasts (30S-30N). Each graph plots the forecast probability versus the observed relative frequency for a given category (above-normal, upper row; below-normal, lower row). Different forecast methods are compared: individual AGCMs (thin black lines); Pooled MM probabilities (heavy grey line); Bayesian MM probabilities (heavy black line). In the left column, the "raw probabilities" from the models are used; in the right column, the "corrected probabilities" are used. The inset graphs show the frequency with which the forecast probabilities were assigned for the Bayesian MM ensemble.

The Predictability Barrier and Teleconnection Pattern Variability

J.S. Frederiksen¹ and G. Branstator²

¹CSIRO Atmospheric Research, Aspendale, Victoria, Australia

²National Center for Atmospheric Research, Boulder, Colorado, USA

Corresponding author: Jorgen.Frederiksen@csiro.au

1. Introduction

Models of climate prediction over the tropical Pacific commonly encounter a predictability barrier in boreal spring when correlations between observations and predictions rapidly decline. Lagged correlations between the mean monthly Southern Oscillation index are also found to decrease rapidly in boreal spring (Webster and Yang, 1992). Recently Frederiksen and Branstator (2001) (hereafter FB1) suggested that a contributing cause of the boreal spring predictability and correlation barrier may be the fact that amplitudes of the large-scale instabilities of the atmospheric circulation have peaks in northern spring. They studied how the inclusion of the annual cycle of basic states affects the properties of leading instability eigenmodes of the barotropic vorticity equation and found dramatic seasonal fluctuations in the growth rates and amplitudes of finite-time normal modes (FTNMs). Low-frequency atmospheric anomalies also exhibit distinct seasonal variability (Branstator and Frederiksen, 2003). The purpose of the present article is to report on results of a study in which we employ an analogous methodology to that of FB1 to study the seasonal variability of teleconnection patterns determined as finite-time principal oscillation patterns (FTPOP) from reanalysed observations. We examine the extent to which finite-time normal mode instability theory is able to provide insights into the structural and amplitude variability of teleconnection patterns as they fluctuate during the annual cycle. We relate teleconnection pattern variability to the predictability barrier.

2. Theory

The FTPOP are the eigenvectors of the propagator obtained by fitting a linear stochastic model to a statistically cyclostationary data set with mean $\bar{\mathbf{x}}(t)$ that is time-dependent and fluctuations about the mean $\mathbf{x}(t)$. Our linear stochastic model has the form

$$\frac{d\mathbf{x}}{dt} = \mathbf{M}(t)\mathbf{x}(t) + \mathbf{f}(t) \quad (1)$$

where $\mathbf{M}(t)$ is a time-dependent matrix to be determined from the data and $\mathbf{f}(t)$ represents noise. The solution to Eq. (1) may then be written as

$$\mathbf{x}(t) = \mathbf{G}(t,0)\mathbf{x}(0) + \int_0^t ds \mathbf{G}(t,s)\mathbf{f}(s) \quad (2)$$

Here $\mathbf{G}(t,s)$ is the propagator which has the integral representation $\mathbf{G}(t,s) = \mathbf{T} \exp \int_s^t d\sigma \mathbf{M}(\sigma)$ (3)

where \mathbf{T} is the chronological time-ordering operator (FB1, Eq.(2.4)). Since our data are only sampled every $\Delta t = 12$ hrs we estimate the stability matrix $\mathbf{M}(t)$ through the associated finite-difference equation. The estimate of \mathbf{M} that minimizes the noise is then given through Gauss' theorem of least squares as

$$\mathbf{M} = \left[\left\langle \mathbf{x}(t + \Delta t)\mathbf{x}^+(t) \right\rangle \left\langle \mathbf{x}(t)\mathbf{x}^+(t) \right\rangle^{-1} - \mathbf{I} \right] (\Delta t)^{-1} \quad (4)$$

where, \mathbf{I} is the unit matrix, $+$ denotes Hermitian conjugate and angular brackets denote ensemble (or time) means. The FTPOP between an initial time $t=0$ and a final time T , taken here to be 1 year, are the eigenvectors of the eigenvalue-eigenvector problem

$$\left(\lambda^v [T,0] \mathbf{I} - \mathbf{G}(T,0) \right) \phi^v [T,0] = 0 \quad v = 1, \dots, N \quad (5)$$

where $\lambda^v = \lambda_r^v + i\lambda_i^v$ are the eigenvalues ϕ^v are the column eigenvectors and N is the total length of the vectors.

3. FTPOP for reanalysed observations

In our case $\mathbf{x}(t)$ is the column vector of spherical harmonic spectral components truncated rhomboidally at wave number 15 and based on twice daily National Centers for Environmental Prediction-National Center for Atmospheric Research reanalysis 300-hPa streamfunction fields. We focus on data from the 40 year period starting on 1 January 1958.

Fig.1a shows two measures of the change with the annual cycle of the root mean square streamfunction amplitude of FTPOP1, the leading (least damped) empirical mode. The first is the local total growth rate $\tilde{\omega}_i^1(t)$ (dashed), the tendency of the logarithm of the amplitude, and the second is the relative amplification factor $R^1(t)$ (thick solid), the ratio of the evolved to initial

amplitudes (scaled by $\exp \omega_i^1 t$ where $\omega_i^1 t$ is the global or annual average growth rate). Comparing this diagram with the corresponding theoretical results in Fig.4a of FB1 for FTNM1 we note a number of general similarities. Firstly the maximum relative amplification factor occurs in early boreal spring and has a magnitude of around twice the value in January. It then plummets in late boreal spring attaining low values in boreal summer and autumn and with generally increasing values in late autumn and early winter. We also note that the minimum in $R^1(t)$ for both FTPOP1 and FTNM1 occurs between October and November. These similarities are also

reflected in the local growth rates. In Fig.1b we show the average local total growth rate of the five leading FTPOPs (in dashed) and the relative amplification factor $R(t)$ in thick solid). The amplification factor again has largest values in the first half of the year (as did the five leading FTNMs in Fig.4b of FB1), decreases rapidly in late boreal spring and summer and then increases gradually in boreal autumn and winter. The growth rates tend to be smallest on average in northern summer, and largest in northern autumn and winter.

Fig.2a shows the 300-hPa disturbance streamfunction for FTPOP1 on 15 January on Northern Hemisphere stereographic projection. FTPOP1 displays the distinct Pacific-North American pattern. By 15 March, FTPOP1 has attained the more zonally symmetric structure shown in Fig. 2b for the Northern Hemisphere. In each month the leading FTPOPs have similar structures to some of the leading empirical orthogonal functions (EOFs), the eigenvectors of the monthly averaged streamfunction covariance matrix, and to leading principal oscillation patterns (POPs), the eigenvectors of the propagator with the monthly averaged empirical stability matrix M (Frederiksen and Branstator, 2005; hereafter FB2).

The structural and amplitude changes of the leading FTPOPs as they evolve (not shown) have a similar complexity to that shown in Fig.5 of FB1 for their FTNM1. The FTPOPs however tend to have larger relative amplitudes in the subtropical regions and in the Southern Hemisphere than do the FTNMs. This may be seen by comparing Fig.3 with Fig.7b of FB1. Fig.3 shows a latitude-time cross section of the zonal average of the absolute value of the 300-hPa streamfunction for FTPOP1 (scaled by $\exp \omega_i^1 t$). We note the fairly comparable amplitudes in the Northern and Southern Hemispheres, particularly during the first half of the year, and the peak amplitudes in March when the equatorial penetration of the disturbance is also the largest. In contrast for FTNM1, in Fig.7b of FB1, the Southern Hemisphere amplitudes are much smaller than Northern Hemisphere amplitudes. These differences arise because the FTPOPs experience interannual sea surface temperature (SST) variability as well as the internal atmospheric processes also seen by FTNMs. Leading FTPOPs for general circulation model simulations without interannual SST variability match more closely the structures of leading FTNMs (FB2).

4. Conclusions

We have found that in many respects the properties of theoretical FTNMs established in FB1 also carry over to their observational counterparts, the FTPOPs. The most striking similarity between FTNMs and FTPOPs is in the seasonality of the growth rates of the leading modes. In both theoretical and empirical settings there is a distinct annual cycle of these rates with the maximum occurring during the middle of the boreal cold season and a broad minimum being present during the boreal warm season.

The similarity in the seasonality of growth characteristics is even more evident if one considers the time-integrated effects of growth, as given by our relative amplification rate. In this case one finds that for both theoretical and empirical modes maximum amplitudes are reached near the end of March and minimum amplitudes occur in early November. A further similarity that we have found between growth properties of leading FTNMs and FTPOPs is that both attain growth rates during each season that are similar to the growth one would expect from normal modes and POPs calculated for that season (not shown). This means that in both cases perturbations are reacting to the seasonally changing basic state faster than the state is changing. In FB1 it was shown that this is only a first approximation, particularly during boreal spring when intermodal growth appears to make a significant contribution, but it serves to explain why linear planetary wave models that employ basic states that are constant in time can be useful.

Both leading FTPOP teleconnection patterns and the leading FTNM instabilities of FB1 have peak amplitudes in boreal spring. These results again suggest a close relationship between the boreal spring predictability barrier of some models of climate prediction over the tropical Pacific Ocean and the amplitudes of the large-scale instabilities and teleconnection patterns of the atmospheric circulation.

References

- Branstator, G. and J.S. Frederiksen 2003: The seasonal cycle of interannual variability and the dynamical imprint of the seasonally varying mean state. *J. Atmos. Sci.*, 60, 1577-1592.
- Frederiksen, J.S. and G. Branstator 2001: Seasonal and intraseasonal variability of large-scale barotropic modes. *J. Atmos. Sci.*, 58, 50-69.
- Frederiksen, J.S. and G. Branstator 2005: Seasonal variability of teleconnection patterns. *J. Atmos. Sci.*, 62, in press.
- Webster, P.J. and S. Yang 1992: Monsoon and ENSO: Selectively interactive systems. *Quart. J. Roy. Meteor. Soc.*, 118, 877-926.

From multi-model ensemble predictions to well-calibrated probability forecasts: Seasonal rainfall forecasts over South America 1959–2001

Caio A. S. Coelho¹, David B. Stephenson¹, Francisco J. Doblas-Reyes², and Magdalena Balmaseda².

¹Department of Meteorology, University of Reading – Reading, U.K.

²ECMWF – Reading, U.K.

Corresponding author: c.a.d.s.coelho@reading.ac.uk

Introduction

South American rainfall seasonal forecasts are currently produced using either physically derived numerical climate models or using empirical (statistical) relationships based on historical data. Only a few studies have compared the skill of these two approaches for some regions of South America, indicating that more comparison studies are required. This paper aims to compare the skill of an empirical model with coupled multi-model December-January-February (DJF) South American rainfall anomaly predictions. The austral summer season is when most of South America receives most of its annual rainfall. Therefore, good quality predictions for DJF are crucial for those sectors that depend on seasonal rainfall for future planning (e.g. agriculture, electricity generation).

Methodology

The multi-model ensemble investigated here is composed of three coupled models (ECMWF, Meteo-France and UKMO), and was produced as part of the DEMETER¹ project. Each model provides 9 members to compose the 27 multi-model ensemble. One-month lead predictions for DJF are investigated. The empirical model uses the previous season August-September-October (ASO) ERA-40² sea surface temperature anomalies of the Pacific and Atlantic as predictors for DJF rainfall anomalies (Chen *et al.*, 2002) for the entire South American continent. The skill of the empirical model is compared to the skill of both the simple multi-model ensemble, obtained by pooling all 27 ensemble members, and the skill of combined/calibrated forecasts obtained using the Bayesian forecast assimilation (FA) procedure as described in Stephenson *et al.* (2004). Coelho *et al.* (2004) and Coelho *et al.* (2003) provide additional information about the Bayesian method of calibration/combination of forecast. All results shown here were obtained using the cross-validation method (Wilks 1995). Skill assessment is performed for the period 1959–2001, which is the common period of hindcasts produced by the three DEMETER coupled models. Additional information about South American DEMETER hindcasts can be found at <http://www.met.reading.ac.uk/~swr01cac>

Results and Discussion

Figure 1 (page 16) shows correlation maps (Figs. 1a-c) and Brier Skill Score (BSS, see Wilks, 1995) maps (Figs. 1d-f) of rainfall anomaly predictions for empirical, multi-model and forecast assimilation (FA) for the period 1959–

2001. These maps show the correlation between observed and predicted anomalies at each grid point. The BSS is for the event 'rainfall anomaly less than or equal to zero'. The BSS represents the level of improvement of the Brier score (Brier, 1950) compared to that of a reference forecast (in this case climatological probability of the event). The BSS is designed to range from one for perfect predictions, through zero for predictions that provide no improvement over the reference forecast, to negative values for predictions that are worse than the reference forecast. The tropical region, in Northern South America, is the most skilful region with correlations between 0.6 and 0.8 and BSS between 0.1 and 0.6. The subtropics (south Brazil, Paraguay, Uruguay and northern Argentina) also show some skill. Correlations between 0.2 and 0.5 are found in this region. These two regions are well known to be influenced by the El Niño Southern Oscillation (ENSO). This suggests that most of the skill of South American rainfall predictions is ENSO derived. Empirical, multi-model and forecast assimilation predictions have similar correlation maps (Figs. 1a-c), indicating that these three approaches have comparable level of deterministic skill. The probabilistic measure of skill (Figs. 1d and 1e) shows that empirical predictions are more skilful than multi-model predictions, particularly in the tropical region where empirical predictions have higher BSS. Bayesian combined/calibrated predictions obtained with forecast assimilation (Fig. 1f) have higher BSS than uncalibrated multi-model predictions (Fig. 1e). This indicates that the calibration provided by forecast assimilation improves the skill of the multi-model predictions. This increase in BSS is mainly due to improvements in the reliability of the predictions, with the tropical regions also showing improvements in resolution (not shown). Combined/calibrated predictions obtained with forecast assimilation (Fig. 1f) have now comparable level of probabilistic skill as empirical predictions (Fig. 1d). The predominance of negative BSS in Figs. 1d-f is due to some properties of this score. Mason (2004) has shown that the expected value of the BSS is less than zero if nonclimatological forecast probabilities are issued. As a result, negative skill scores can often hide useful information content in the forecasts. Therefore, negative skill scores need to be interpreted with caution.

Figure 2 (page 20) shows the mean anomaly correlation coefficient (ACC) for La Niña, neutral and El Niño years occurring during 1959–2001 (Table 1 Page 18) and all years. The ACC of each year is given by the correlation between the observed and predicted spatial anomaly

Continued on page 19

¹ <http://www.ecmwf.int/research/demeter>

² <http://www.ecmwf.int/research/era>

From Philippon et al. Page 5: Preliminary study of the East African short rains predictability at the monthly and grid-point scales (1968-1998)

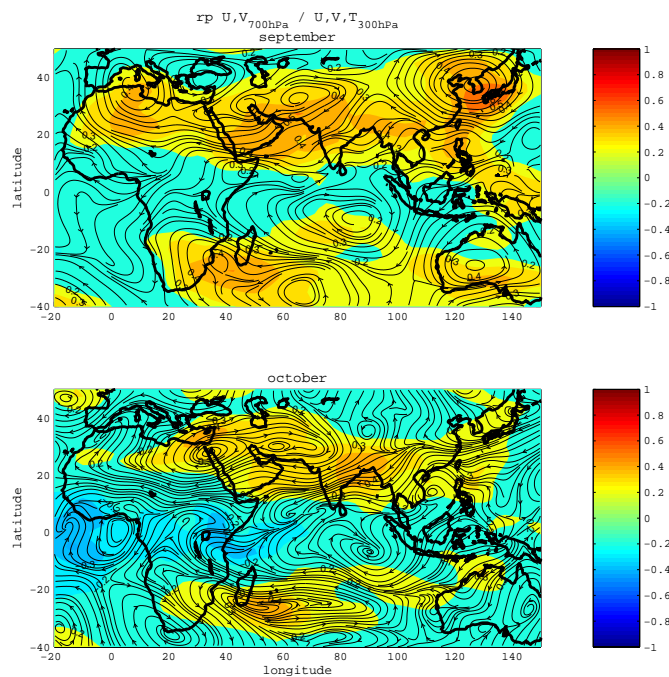


Figure 5: correlation maps between the October wind expansion coefficient and (a) September, (b) October 300hPa temperature (colour shading) and streamfunction, independently from 'PCO', 'V200' and 'MDI'.

From Goddard et al. Page 8: Multi-Model ensembling: Refining and Combining

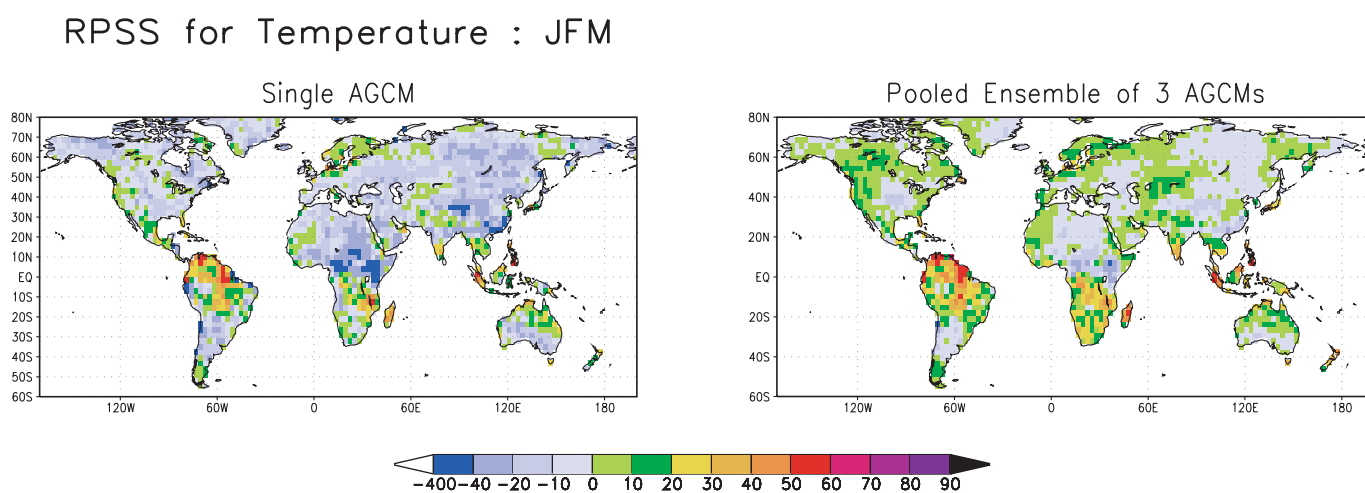


Figure 1. Maps of Ranked, Probability Skill Score (RPSS) for 3-category JFM temperature forecasts over the period 1950-95. (Left) individual AGCM ensemble; (Right) pooled combination of the raw AGCM probabilities, which is considered the "baseline" approach for the multi-model ensemble combination.

From Coelho et al. Page 14: From multi-model ensemble predictions to well-calibrated probability forecasts: Seasonal rainfall forecasts over South America 1959-2001

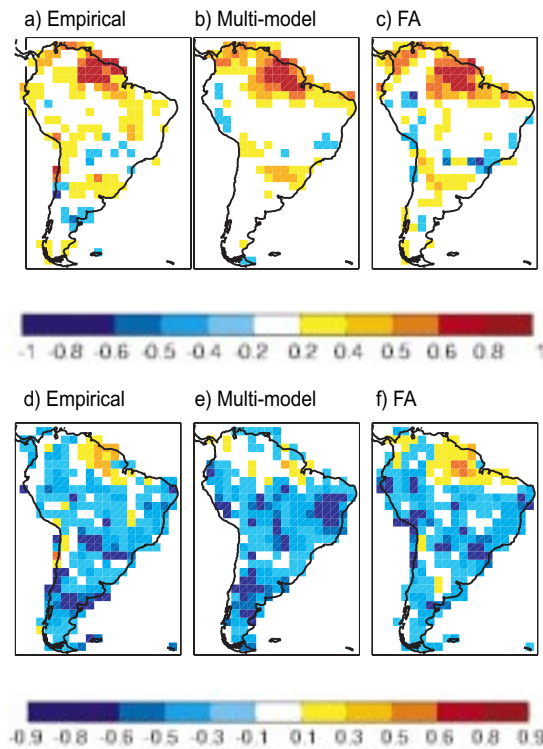


Figure 1: Correlation maps (panels a-c) and Brier Skill Score maps (panels d-f) of empirical, multi-model and forecast assimilation (FA) DJF predictions for the period 1959-2001

From Cavalcanti et al Page 23: Seasonal climate prediction over South America using the CPTEC/COLA AGCM

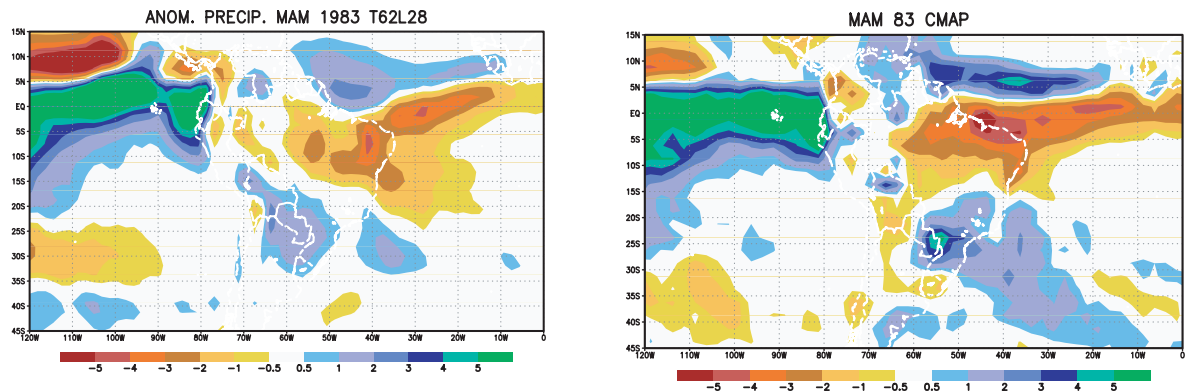


Fig.1. Precipitation anomalies in MAM 1983 (a) AGCM; (b) CMAP

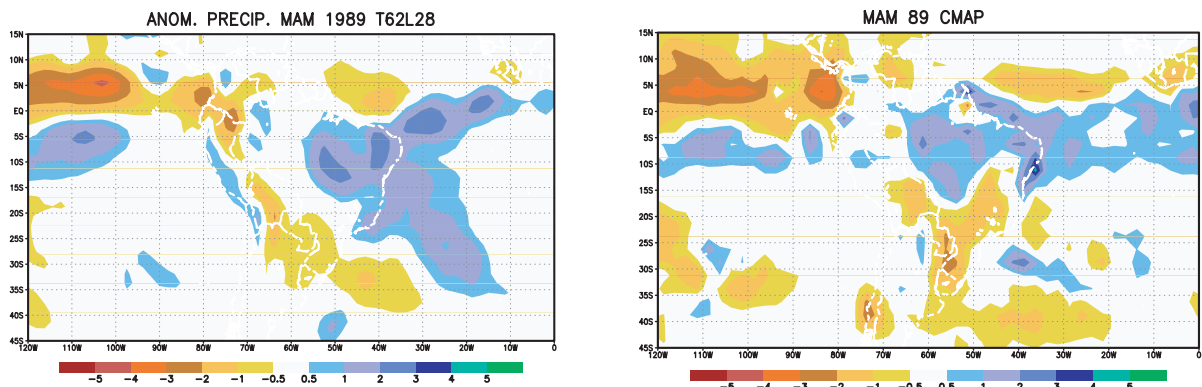


Fig.2. Precipitation anomalies in MAM 1989 (a) AGCM; (b) CMAP

From Berri et al Page 25: Seasonal Precipitation Forecasts for the Southeast of South America. Evaluating the First Five Years

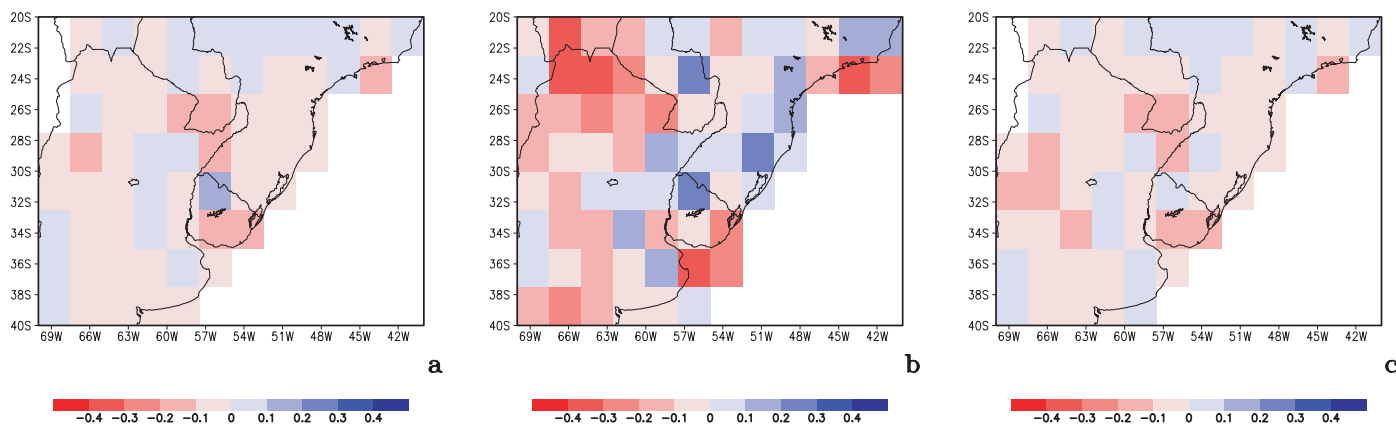


Figure 2 a) averaged skill score S of 16 COF seasonal precipitation forecast; b) averaged skill score S of 13 IRI seasonal precipitation forecasts (see text for details); c) averaged skill score S of COF seasonal precipitation forecast for the same 13 periods as b). The period of analysis is 1998-2002.

From Kripalani et al. Page 27: Are Intra-seasonal oscillations "Speed-breakers" to Seasonal Prediction?

3-7 days mode

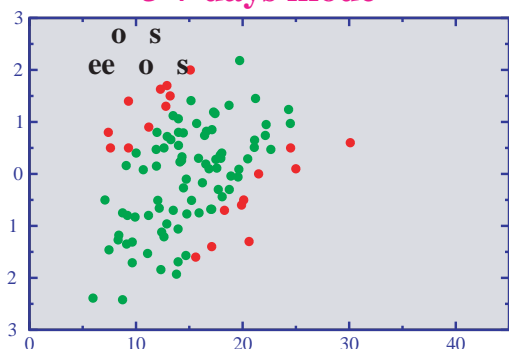


Fig.1 : Scatter plot of the inter-annual monsoon variability (standardized IMR) and the intensity of the 3-7 days mode (variance in percentage). Points that do not satisfy the relationship are shown as red dots (so-called Speed-breakers). CC=Correlation Coefficient between intensity of mode and IMR.

10-20 days mode

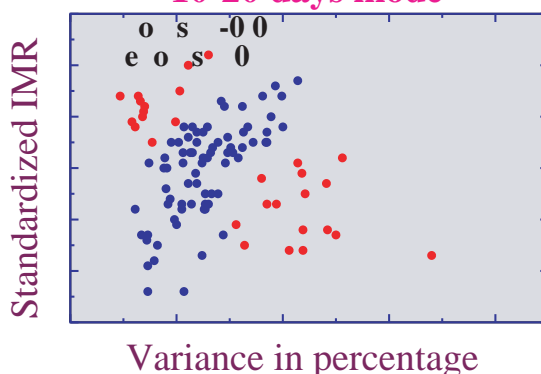


Fig. 2: Same as Fig. 1 but for the 10-20 days mode

30-60 days mode

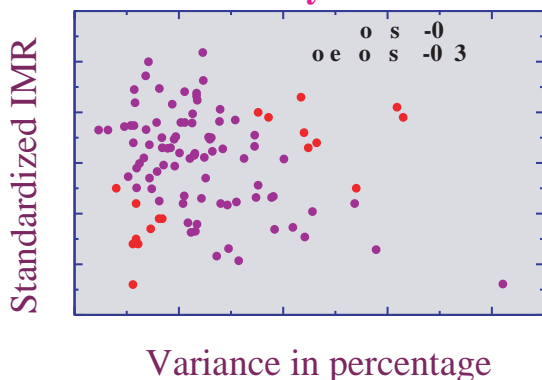


Fig. 3: Same as Fig. 1 but for the 30-60 days mode

PAGES 2nd Open Science Meeting

10-12 August 2005

Beijing, China



Paleoclimate, Environmental Sustainability and our Future

Meeting themes

- Future Change: Historical Understanding
- Humans and their Environment: Past Perspectives on Sustainability
- Ocean-Continent-Cryosphere Interactions: Past and Present
- Climate, Humans and the Environment in the Asian Region
- PAGES Research Foci and Initiatives within IGBP

The OSM will consist of plenary lectures and poster sessions.
See the final program at www.pages2005.org/schedule.html

The PAGES OSM is being held alongside the 9th IAMAS Scientific Assembly (2-11 August 2005).

Poster abstract deadline:
31 March 2005

Early Registration before:
15 May 2005

GLOBAL
I G B P
CHANGE

www.pages2005.org

PAGES
PAST GLOBAL CHANGES

From Coelho et al Page 14: From multi-model ensemble predictions to well-calibrated probability forecasts: Seasonal rainfall forecasts over South America 1959-2001

	Years
La Niña	1964/65, 1970/71, 1971/72, 1973/74, 1974/75, 1975/76, 1983/84, 1984/85, 1988/89, 1995/96, 1998/99, 1999/00, 2000/01
Neutral	1959/60, 1960/61, 1961/62, 1962/63, 1966/67, 1967/68, 1978/79, 1980/81, 1981/82, 1985/86, 1989/90, 1993/94, 1996/97, 2001/02
El Niño	1963/64, 1965/66, 1968/69, 1969/70, 1972/73, 1976/77, 1977/78, 1979/80, 1982/83, 1986/87, 1987/88, 1990/91, 1991/92, 1992/93, 1994/95, 1997/98

Table 1: La Niña, neutral and El Niño years occurring during 1959-2001.

Continued from page 14

pattern. La Niña and El Niño years have higher mean ACC than neutral years, indicating that predictions for ENSO years are more skilful than predictions for neutral years. El Niño and La Niña predictions obtained with forecast assimilation show an increase in the mean ACC compared to the uncalibrated multi-model. The mean ACC of El Niño and La Niña forecast assimilation predictions are now comparable to the mean ACC of empirical predictions. Neutral years have nearly null mean ACC, indicating that rainfall anomalies of these years are hardly predicted.

Figure 3 (page 20) shows observed and predicted composites of DJF rainfall anomalies for those La Niña and El Niño years listed in Table 1. Figures 3b and 3f show that the empirical model reproduces remarkably well both La Niña and El Niño observed composites patterns (Figs. 3a and 3e). The correlation between the predicted and observed patterns is 0.95 for the La Niña composite and 0.97 for the El Niño composite. The multi-model composites (Figs. 3c and 3g) partially reproduce the observed pattern in equatorial South America and fail to reproduce the observed pattern in the other regions of the continent. The correlation between the multi-model composite and the observed composite is 0.28 for La Niña and 0.51 for El Niño. Bayesian combined/calibrated composites produced with forecast assimilation (Figs. 3d and 3h) are in much better agreement with the observations. The correlation between FA composites and observed composites is 0.82 for La Niña and 0.97 for El Niño, being now comparable to the correlation values of empirical composites. These results suggest that additional skill can be gained by calibrating multi-model predictions with forecast assimilation.

Conclusions

This study addressed seasonal predictability of South American rainfall. The skill of empirical, DEMETER coupled multi-model and combined/calibrated predictions obtained with forecast assimilation has been assessed and compared. This comparison revealed that when seasonally forecasting Dec-Jan-Feb South American rainfall at 1-month lead-time the current generation of coupled models have comparable level of skill to those obtained using a simplified empirical approach. The same conclusion still holds for longer (e.g. 3-month) lead times. This result is in agreement with findings of previous comparison studies.

Bayesian forecast assimilation has been shown to be a powerful tool for the calibration of multi-model predictions. Forecast assimilation predictions have been shown to have improved BSS compared to the simple multi-model prediction. This is because forecast assimilation provides better estimates of forecast uncertainty than coupled multi-model. Forecast assimilation predictions (and FA alone) produce probability forecasts with skill in Southeastern South America – an important region for hydroelectricity production. Additionally, forecast assimilation ENSO

composites have been shown to be in much better agreement with observed composites than multi-model composites.

The tropics and the area of south Brazil, Paraguay, Uruguay and northern Argentina have been found to be the two most predictable regions of South America. South American rainfall is generally only predictable in ENSO years rather than in neutral years, which exhibit very little skill.

Acknowledgements

CASC was sponsored by Conselho Nacional de Desenvolvimento Científico e Tecnológico (CNPq) process 200826/00-0. FJDR was supported by DEMETER (contract EVK2-1999-00024).

References

- Brier, G. W., 1950: Verification of forecasts expressed in terms of probability. *Mon. Wea. Rev.*, 78, 1-3.
- Chen, M., P. Xie, J. E. Janowiak, and P. A. Arkin, 2002: Global land precipitation: A 50-yr monthly analysis based on gauge observations, 2002, *J. of Hydrometeorology*, 3, 249-266.
- Coelho, C. A. S., S. Pezzulli, M. Balmaseda, F. J. Doblas-Reyes and D. B. Stephenson, 2003: Skill of coupled model seasonal forecasts: A Bayesian assessment of ECMWF ENSO forecasts. *ECMWF Tech. Memo.* 426.
- Coelho, C. A. S., S. Pezzulli, M. Balmaseda, F. J. Doblas-Reyes and D. B. Stephenson, 2004: Forecast calibration and combination: A simple Bayesian approach for ENSO. *J. Climate.*, 17, 1504-1516.
- Mason, S. J., 2004: On Using "Climatology" as a Reference Strategy in the Brier and Ranked Probability Skill Scores. *Monthly Weather Review.* 132, 1891-1895
- Stephenson D. B., C.A.S. Coelho, F. J. Doblas-Reyes and M. Balmaseda, 2004: Forecast Assimilation: A unified framework for the combination of multi-model weather and climate predictions. *Tellus A – DEMETER special issue* (in press).
- Wilks, D. S., 1995: Statistical methods in atmospheric sciences: An introduction. 1st Edition. Academic Press. 467pp.

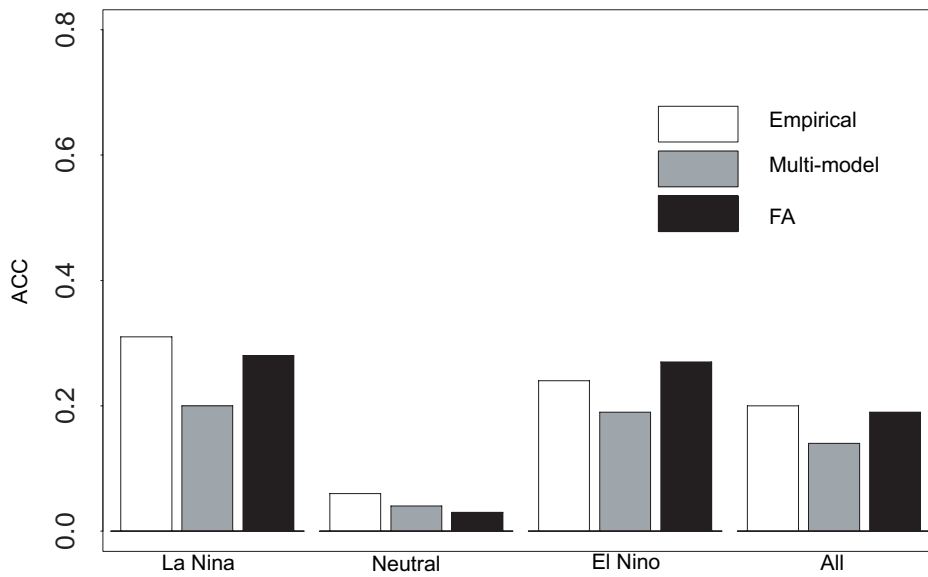


Figure 2: Mean ACC for empirical, multi-model and forecast assimilation (FA) predictions of La Niña, neutral and El Niño years of Table 1 and all (1959-2001) years.

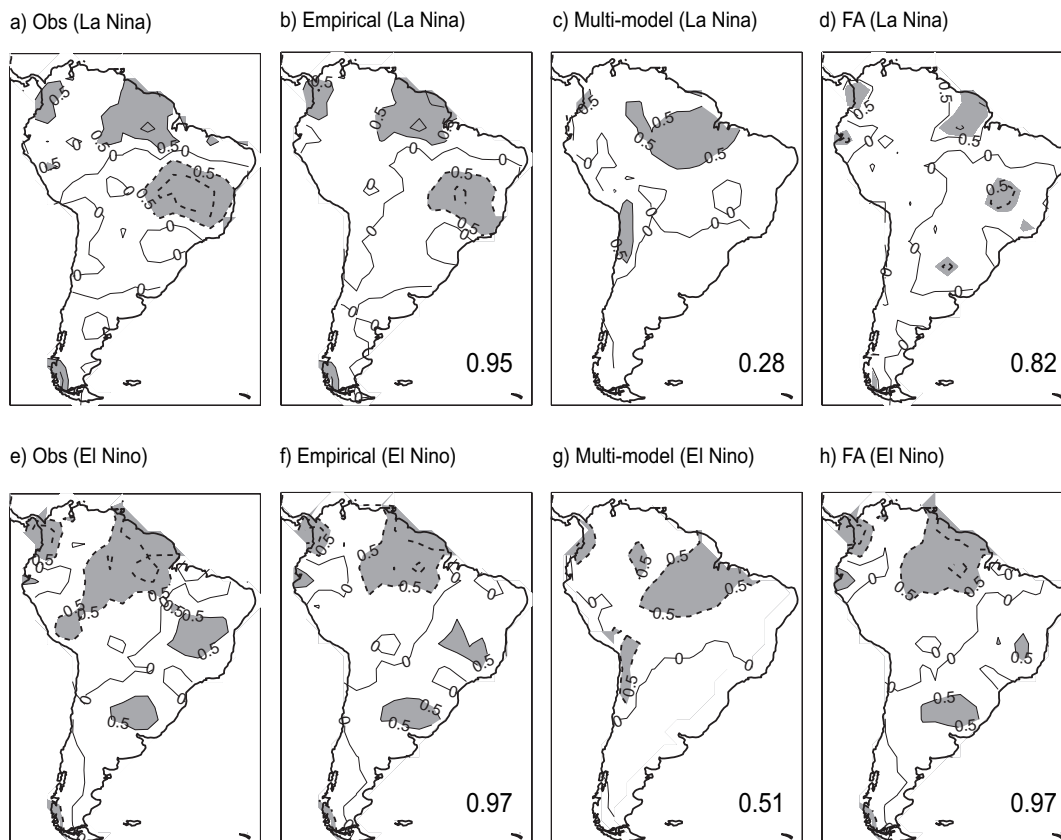


Figure 3: Observed (panels a and e) and predicted (panels b-d and f-h) DJF rainfall anomaly composites of La Niña and El Niño years (in mm.day⁻¹) by empirical, multi-model and forecast assimilation (FA). The number in the bottom right hand corner of panels b-d) and f-h) is the correlation between the observed composite and the predicted composite. Contour interval is 0.5 mm.day⁻¹. Rainfall anomalies below -0.5 mm.day⁻¹ and above 0.5 mm.day⁻¹ are grey shaded.

Seasonal Forecast of Antarctic Sea Ice

Dake Chen and Xiaojun Yuan

Lamont-Doherty Earth Observatory of Columbia University, Palisades, New York

Corresponding author: dchen@ldeo.columbia.edu

1. Introduction

Long-range forecasts of Antarctic sea ice are very much in demand, not only because of the potential importance of sea ice in global climate, but also for the practical purpose of exploring the Antarctic continent. Unfortunately, such forecasts are not yet feasible with any state-of-the-art general circulation models, because the complex air-sea-ice interaction processes on long timescales are still not well understood and are by no means well simulated by these models. An alternative is to apply statistical methods to Antarctic sea ice prediction. The linear Markov model used in this study (Chen and Yuan, 2004) represents one of the first attempts in this direction.

The variability of Antarctic sea ice is likely to be controlled by both remote and local processes. The atmospheric anomalies from low latitudes could excite certain modes of the Antarctic climate system, which then could be amplified and sustained by the local air-sea-ice interaction. Here we explore the possibility of forecasting Antarctic sea ice anomalies using a technique combining multivariate empirical orthogonal function (MEOF) analysis and linear Markov prediction. Our model results indicate that the dominant modes of the Antarctic climate variability is indeed predictable up to one year in advance, and that our simple statistical model can serve as a useful tool for Antarctic sea ice prediction until better dynamical models come along.

2. Model and Data

Our model is constructed in the MEOF space. In other words, the base functions of the model's spatial dependence consist of the MEOFs of several variables that are chosen to define the state of the Antarctic climate, while the temporal evolution of the model is a Markov process with its transition functions determined from the corresponding principal components (PCs). By retaining only a few leading modes of the MEOFs, we can greatly reduce the model space and, more importantly, filter out incoherent small-scale features that are basically unpredictable. This kind of model has been used previously in some ENSO predictability and prediction studies (Blumenthal, 1991; Xue et al., 2000; Canizares et al., 2001).

We chose to define the coupled Antarctic climate system with eight variables: sea ice concentration, surface air temperature, sea level pressure, zonal and meridional surface winds, 300mb geopotential height, and zonal and meridional winds at 300mb level. The sea ice data were obtained from the National Snow and Ice Data Center and then binned into $0.5^\circ\text{lat} \times 2^\circ\text{long}$ grids and monthly

intervals. All other data sets came from the reanalysis product of the National Center for Environmental Prediction, which are monthly data on a $2.5^\circ \times 2.5^\circ$ grid. The model domain covers the southern polar region ($50\text{--}90^\circ\text{S}$). Twenty-two years (01/1979-12/2000) of observational and reanalysis data were used in this study. The details of model construction can be found in Chen and Yuan (2004).

3. Results

Hindcast experiments were carried out for the period from January 1979 to December 2000. The Markov model was initialized with observational and reanalysis data in each month and predictions were made for up to 12 months for all model variables. The model showed remarkable skill in predicting the Antarctic dipole, the dominant mode of climate variability in the southern polar region (Yuan and Martinson, 2001), especially in austral winter (JJA). As an example, Figure 1 (front cover) displays the model hindcasts at different lead times for the winter of 2000, when a typical dipole pattern occurred in response to the 1999-2000 La Niña. The top row (0-month lead) is simply the observations represented by the first 7 MEOF modes and thus can be considered as the target. The model did a fairly nice job predicting all of the main features in the observed sea ice and atmospheric variables, though the prediction made 9-months ahead is a bit weak in magnitude.

To prevent artificial skills, the model was evaluated using a cross-validation scheme (Barnston and Ropelewski, 1992), in which the data used to verify the model hindcasts are not used for model training. Figure 2 (page 22) shows the cross-validated model skills in predicting the average sea ice anomaly at DP1 ($130\text{--}150^\circ\text{W}$, $60\text{--}70^\circ\text{S}$, the center of the dipole in Pacific). The model beats the persistence prediction by a large amount in terms of both anomaly correlation and rms (root-mean-square) error. Among the four model cases with different numbers of MEOF modes included, the one with 7 modes has the highest overall score. In this case, the anomaly correlation is above 0.6 and the rms error is below 9% for almost all lead times up to almost one year. It is worth noting that the model is not particularly sensitive to the number of modes retained.

We started real-time seasonal forecasting of Antarctic sea ice in the beginning of 2003. Since then we have been providing forecasts on a monthly basis in our experimental sea ice prediction webpage (http://rainbow.ldeo.columbia.edu/~dchen/sea_ice.html) at Lamont-Doherty Earth Observatory of Columbia University. So far the forecast results are quite

encouraging. The gross features of our model predictions have been verified by recent observations.

4. Summary and Discussion

We have developed a low-order linear Markov model to simulate and predict the short-term climate change in Antarctic, with particular emphasis on sea ice variability. Seven atmospheric variables along with sea ice were chosen to define the state of the Antarctic climate, and the multivariate empirical orthogonal functions of these variables were used as the building blocks of the model. In both hindcast and forecast experiments, the model showed considerable skill in predicting the Antarctic sea ice anomalies up to a year in advance, especially in austral winter and in the Antarctic dipole regions. We are presently using this model for experimental seasonal forecasting of Antarctic sea ice, which is expected to be useful for planning Antarctic field expeditions.

It is somewhat surprising that such a simple statistical model could have fared so well in predicting the interannual variations of the Antarctic sea ice field, a task that has rarely been attempted before. The predictability demonstrated here can be attributed to the domination of the coupled air-sea-ice system by a few distinctive, slowly-changing modes such as the Antarctic dipole, although a self-sustained low-frequency oscillation is not likely to exist in Antarctic. Our understanding of the physical processes operating in the Antarctic climate system is still rather limited, but we do have a good grasp of the statistical characteristics of the system, and a well-constructed statistical model can be a useful forecast tool as long as it contains those dominant climate modes.

This self-evolving Markov model emphasizes the regional air-sea-ice interaction, and as such it does not explicitly simulate the Antarctic-low-latitude teleconnection. However, the success of the model does not compromise in any way the importance of the teleconnection. Since the Antarctic interannual disturbances are likely to be excited in the first place by the influence from low latitudes, as evident in their lagged response to ENSO, any models that simulate the evolution of these disturbances implicitly take into account the teleconnection. What the model does is nothing but to pick out significant signals from observed initial conditions and predict a statistically meaningful path for the movement, growth, or decay of these initial disturbances.

Acknowledgements.

This research is supported by the National Aeronautics and Space Administration through grant NAG5-12587.

References:

- Barnston, A. G., and C. F. Ropelewski, 1992: Prediction of ENSO episodes using canonical correlation analysis. *J. Clim.*, 5, 1316-1345.
- Blumenthal, M. B., 1991: Predictability of a coupled ocean-atmosphere model. *J. Clim.*, 4, 766-784.

- Canizares, R., A. Kaplan, M. A. Cane, D. Chen, and S. E. Zebiak, 2001: Use of data assimilation via linear low order models for the initialization of ENSO predictions. *J. Geophys. Res.*, 106, 30947-30959.
- Chen, D. and X. Yuan, 2004: A Markov model for seasonal forecast of Antarctic sea ice. *J. Clim.*, 17, 3156-3168.
- Xue, Y., A. Leetmaa and M. Ji, 2000: ENSO prediction with Markov models: the impact of sea level. *J. Clim.*, 13, 849-871.
- Yuan, X. and D. G. Martinson, 2001: The Antarctic Dipole and its Predictability. *Geophys. Res. Lett.*, 28, 3609-3612.

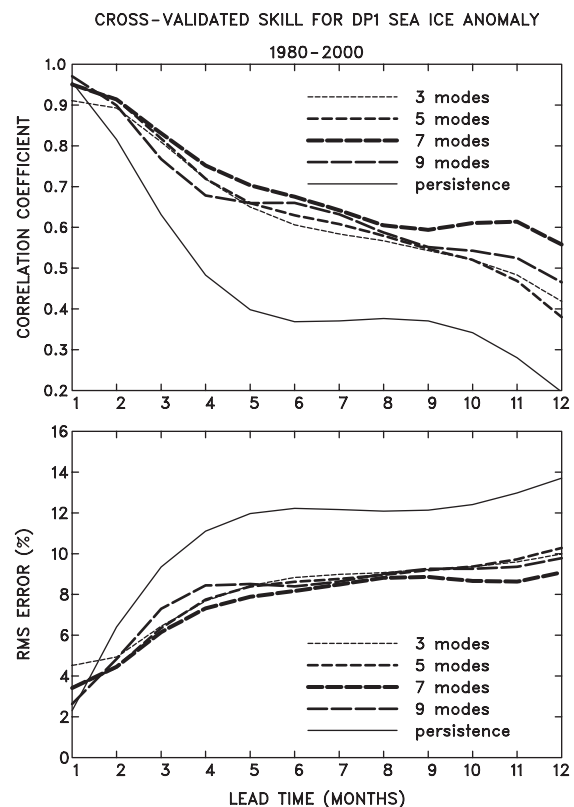


Figure 2. Cross-validated correlation and rms error between hindcast and observed sea ice concentration anomalies averaged in DP1 region (130-150°W, 60-70°S). Compared are four model hindcast experiments with different numbers of MEOF modes included. The skill of persistence prediction is also shown for reference.

Seasonal climate prediction over South America using the CPTEC/COLA AGCM

Iracema Fonseca de Albuquerque Cavalcanti and José Antonio Marengo;
Center for Weather Forecasting and Climate Prediction/ National Institute for Space Research; Cachoeira Paulista, S.P. Brazil.

Corresponding e-mail: iracema@cptec.inpe.br

Seasonal climate predictability of several regions of South America, using the CPTEC/COLA AGCM, has been assessed through several statistical analyses, studies from model simulations, and through the experience of ten years of applying this model in climate prediction at CPTEC. The AGCM is a spectral model, a version of the Center for Ocean-Land and Atmospheric Studies (COLA) atmospheric model, and has been used with T62L28 resolution in seasonal prediction and climate simulations. The model description can be found in Kinter et al (1997) and Cavalcanti et al (2002).

Results from climate simulations have shown the ability of the AGCM to represent the main global climatological features and the seasonal variability (Cavalcanti et al, 2002). Some typical features of the precipitation field such as the high values of the main convergences zones in the tropics and Southern Hemisphere (ITCZ, SACZ, SPCZ, SICZ), and in the regions of storm tracks of the Northern Hemisphere, and features such as the subtropical jetstreams, subtropical highs, vertical structure of wind and temperature, stationary waves, were well represented by the model.

Regional South American features and statistical analyses from the AGCM results were demonstrated in Marengo et al (2003). The interannual variability of precipitation anomalies for the rainy season of several regions of South America were analysed considering results of 9 integrations with different initial conditions. High convergence among the ensemble members was found for the Northern and Northeast regions and higher dispersion among members in Central and Southeastern Brazil. ROC diagrams which measure the rate of hits and failures showed the highest scores in the Northeast region. This is also the region with high values of reproducibility and anomaly correlations (Cavalcanti et al, 2002; Marengo et al, 2003). Anomaly correlations of precipitation between model results and observations from 1982 to 1991, showed that in all seasons there are high correlation values in the Northern and Northeastern regions and part of the southern region, and low or negative values in large areas of the southeastern region (Marengo et al, 2003). Although the precipitation anomalies are not well simulated over southeastern Brazil, the seasonal cycle and the interannual variability, are very well reproduced by the model, showing a systematic underestimation in the Amazon and southern Brazil regions.

Seasonal prediction has been performed monthly at CPTEC using the CPTEC/COLA AGCM, in an ensemble

mode (Cavalcanti et al, 2000). Two ensembles are constructed with 15 different initial conditions each and two fields of boundary forcing conditions. Persisted Sea Surface Temperature (SST) anomaly is applied to one set, and predicted SST in the tropical Pacific and Atlantic Oceans is applied to the other. Predicted Pacific SSTs are obtained from NCEP and the predicted Atlantic Ocean SST is obtained from a statistical model, SIMOC (Repelli and Nobre 2004, Pezzi et al. 1998). Although the model is global, focus is given to South America and specific areas which require climate attention, as Northeast (NE) and Southern Brazil due to droughts and floods. Fortunately, these are the regions which have the highest predictability in South America.

The influence of the two ENSO phases on precipitation over South America is well simulated and predicted by the AGCM, mainly over Northeast and Southern South America. Examples during the period of ten years simulation are shown in Figs.1 and 2 (Page 16). The CMAP precipitation dataset (Xie and Arkin, 1997) was used for comparisons. Negative anomalies in MAM 83 and positive anomalies in MAM 89 over northeastern Brazil were well simulated. During these periods the opposite anomalies over southern Brazil were also well compared with the observations. In 82/83 floods occurred in Southern Brazil, and the model simulated high positive anomalies over the region. In 88/89 the region experienced dry periods which were well represented by the model. Thus, the confidence on the model is very high during these periods of ENSO in these regions. The model responds very well when the SST anomalous forcing is very strong. In other years, the general pattern over Southern Brazil is not well reproduced, however, considering individual members, some of them are able to represent the anomalies.

Features of the South America monsoon, which comprises areas of the southeastern Brazil, are well represented by the model. The climatological precipitation and wind fields at low and high levels of the summer season are typical of this season and differ completely of those in the winter. The Bolivian High and the Upper Atlantic Trough are well represented by the model, as well as the position of the Atlantic Subtropical High which affects the direction of the trade winds over the northeast Brazilian coast. Other features are typical of the summer season, such as the occurrence of SACZ and different ITCZ position compared to that in the winter. In the summer the ITCZ is located between 0 and 5° N, and in the winter is between 5° and 10° N. These are features which compare well to the observations. Large

seasonal differences occur also in the wind flow at high levels. There are strong westerlies over South America, in the winter, while in the summer there is anticyclonic circulation associated with strong divergence at high levels.

However, Southeastern Brazil (SE) is the region which has the worst predictability over South America. This is a transition region, between the tropical regime to the north (northeast), which has high predictability, and the extratropical regime to the south, which has medium predictability. The low predictability of the Southeastern Brazil can also be related to the different positions of the frontal systems that affect the region in the daily results, in each integration. When the ensemble mean is taken, the features associated with frontal system disappear. However, when analysis of individual ensemble members are considered, features of the frontal systems are well reproduced (Cavalcanti and Coura Silva, 2003). Another reason for the inability of the model to predict precipitation anomalies over Southeastern Brazil, could be related to the use of an atmospheric model with prescribed SST, which does not allow the interaction between the atmosphere and ocean.

Model development concerning the radiation and convection parameterization schemes, updated vegetation, more realistic soil moisture and variable CO₂ are in progress at CPTEC to improve the seasonal predictions. Studies using the Eta regional model in seasonal prediction are in development at CPTEC to depict, in a higher resolution, the regional features over South America. Another future action is the use of a coupled atmosphere-ocean global circulation model in order to include the interaction between SST and the atmosphere, which has a large importance in the subtropical and extratropical regions. Currently, CPTEC is developing a coupled atmospheric-oceanic model that is the state of the art in coupled modeling. It includes the general coupling (without flux correction) of atmospheric CPTEC/COLA AGCM (T62L28 resolution, with the RAS cumulus parameterization scheme) with the MOM_3 global oceanic circulation model of the NOAA Geophysical Fluid Dynamics Laboratory. The coupled model is being tested for the generation of SST and precipitation forecasts.

A suggestion to overcome the problem of simple ensemble technique, in regions with large dispersion, is to use cluster analysis of the ensemble members. Statistical and other analyses of climate variability are being conducted using another dataset resulting from a climate simulation of 50 years.

Lastly, as part of the modeling and development activities at CPTEC, and in the context of programs such as GEWEX and CLIVAR, we have started studies on the issues of predictability, not just applicable to seasonal precipitation forecasts but also to hydrological predictability. We want to address issues like those proposed in the GEWEX and CLIVAR programs. Studies

on the South American Monsoon System are also under development. It is important to consider that Ensemble forecast techniques are beginning to be used for hydrological prediction by operational hydrological services throughout the world. These techniques are attractive because they allow effects of a wide range of sources of uncertainty on hydrological forecasts to be accounted for. The issue of predictability extremes is also very important, and we are focusing on simulations of "climate events" at interannual, intraseasonal and seasonal time scales.

Acknowledgements:

To FAPESP, CNPq and IAI Prosul-CRN055.

References

- Cavalcanti, I.F.A., J.A.Marengo, H. Camargo, C.A.C. Castro, M.B.Sanches, G.O.Sampaio, 2000: Climate prediction of precipitation for the Nordeste rainy season of MAM 2000. *Experimental Long-Lead Forecast Bulletin*, 9, No. 1.
- Cavalcanti, IFA, J.A.Marengo, P.Satyamurty, C.A Nobre, I. Trosnikov, J.P. Bonatti, A.O. Manzi, T. Tarasova, L.P. Pezzi, C. D'Almeida, G. Sampaio, C.C. Castro, M. B. Sanches, H.Camargo, 2002: Global climatological features in a simulation using CPTEC/COLA AGCM. *J.Climate*, 15, 2965-2988.
- Cavalcanti, IFA, L.H. Coura da Silva, 2003: Seasonal Variability over Southeast Brazil related to frontal systems behaviour in a climate simulation with the AGCM CPTEC/COLA. *14th Symposium on global change and climate variations*. AMS Conference, Long Beach, 2003.
- Kinter, III.J.L., D. DeWitt, P.A. Dirmeyer, M.J. Fennessy, B.P. Kirtman, L. Marx, E.K. Schneider, J. Shukla, D. Straus, 1997: The COLA atmosphere-biosphere general circulation model, Vol.1: Formulation. *Report n^o.51, COLA*, Maryland, 46 pp.
- Marengo, J.A., I.F.A. Cavalcanti, P.Satyamurty, I. Troniskov, C.A. Nobre, J.P. Bonatti, H.Camargo, G.Sampaio, M.B. Sanches, A.O. Manzi, C.C. Castro, C.D'Almeida, L.P. Pezzi, L. Candido, 2003: Assessment of regional seasonal rainfall predictability using the CPTEC/COLA atmospheric GCM. *Climate Dynamics*, 21, 459-475.
- Pezzi, L.P., C.A.Repelli, P.Nobre, I.F.A. Cavalcanti, G.Sampaio, 1998: Forecasts of Tropical Atlantic SST anomalies using a statistical Ocean Model at CPTEC/INPE Brazil. *Experimental Long-Lead Forecast Bulletin*, 7, n^o 1, 28-31.
- Repelli, C., P. Nobre, 2004: Statistical Prediction of Sea Surface Temperature over the Tropical Atlantic; *I. J. Climatology*, 24, 34-44
- Xie, P., P.A. Arkin, 1997: Global precipitation: A 17-year monthly analysis based on gauge observations, satellite estimates, and numerical model outputs. *Bull. Amer. Meteor. Soc.* 78, 2539-2558.

Seasonal Precipitation Forecasts for the Southeast of South America. Evaluating the First Five Years

G Guillermo J. Berri* and Pablo L. Antico

Department of Atmospheric and Oceanic Sciences, University of Buenos Aires, Argentina

*Member of the National Research Council of Argentina (CONICET)

Corresponding author: berri@at.fcen.uba.ar

1. Introduction

At the end of 1997, in the middle of the last strong El Niño, a series of Climate Outlook Forums (COFs) began in Southeast of South America. A total of twenty meetings for this region - encompassed by Argentina, Brazil, Paraguay and Uruguay - have been conducted since then. The motivation was the concern about the ongoing El Niño in mid 1997, the availability of experimental climate forecasts, and the knowledge about the impact of past El Niño events in the region. Participation in the COFs included researchers in meteorology, agriculture, hydrology, oceanography and related environmental sciences, and on occasions, in public health and social sciences. The user community was always avid for information about the upcoming climate conditions, so the meetings were attended by a significant number of users of agriculture, water resources management, hydroelectricity generation, civil defense and emergencies. The meetings were sponsored and funded by different international organizations and research institutions, as well as universities, research institutes and research centers in the region, national weather services and water resources centers. For some of the meetings funding was received from hydropower plants, national and regional rural societies and other national and regional organizations.

2. The COFs Forecast

The COFs forecasts consist of a probabilistic tercile distribution -identified as above-normal, normal, below-normal- of the total precipitation and mean temperature expected for the upcoming 3-month period, over a domain in South America between 20°S and 40°S, to the east of the Andes Mountains. The forecast is the result of the consensus agreement between atmosphere model predictions, physically based statistical model predictions, results of diagnostic analysis and published research on climate variability over the region, and expert interpretation of this information in the context of the current situation. The different pieces of information were analyzed and discussed in detail, although the subjective component was always strong because no objective methodology was established. Unpublished research and extrapolation of synoptic experience to the seasonal outlook was also prominent at the COF discussions. Figure 1 (page 26) shows the region of the COFs and the example of a forecast, in which the box over the upper right corner indicates from top to bottom a 25%, 35% and 40% probability of above-normal, near-normal and below-normal precipitation, respectively.

3. Forecast Validation

The first 16 seasonal precipitation forecasts (1998-2002)

are verified using the NOAA CMAP and CAMS-OPI precipitation data with a 2.5-degree resolution. The precipitation data are converted into terciles, based on the precipitation data of New et al. (1999), with the climatology period 1961-1990. Although it is always advisable to use only one data set, it was unavoidable to use different datasets since the available precipitation data used to validate the forecasts does not extend back far enough to define the climatology. For the validation of the forecast we use the *ranked probability skill score S*, a verification measure that takes into account the probability assigned to every category, relative to climatology, defined as $S = 1 - (R / R_{clim})$, where R is the *ranked probability score* defined as:

$$R = \sum_{m=1}^3 (P_m - O_m)^2, \quad P_m = \sum_{j=1}^m p_j, \quad O_m = \sum_{j=1}^m o_j,$$

p_j is the probability assigned to the j th category, P_m is the cumulative forecast vector, O_m is the cumulative observation vector for the first m categories with probabilities o_j , and R_{clim} is obtained by assigning 33% probability to every category. The skill score S is an appropriate measure to qualify a probabilistic forecast, since the magnitude of the error depends on the probabilities assigned to the different categories. A perfect forecast would assign a probability equal to 1 to the category that is observed, and a probability equal to 0 to the other two categories, and thus $R = 0$ and $S = 1$. If the forecast departs from perfection, $R > 0$ and $S < 1$. The minimum acceptable value should be $S = 0$, since S becomes negative when $R > R_{clim}$ so that the forecast is worse than chance (equal probability for every category), and therefore it does not add value.

4. Results

Figure 2a (page 17) shows the mean value of S for the first 16 COFs seasonal precipitation forecasts. In the regions where S is positive, the forecasts perform better than climatology and the overall result could be considered as potentially useful for applications. Such areas are located over NE Argentina, the extreme NW of Uruguay and parts of southern Brazil. This region is approximately coincident with that for which different authors have reported statistically significant correlations between ENSO and precipitation variability on seasonal time scales. It should be stressed that the analyzed period is characterized by strong sea surface temperature anomalies in the tropical Pacific Ocean, which have a significant influence on climate variability over Southeast South America. During most of the analyzed period, 1998

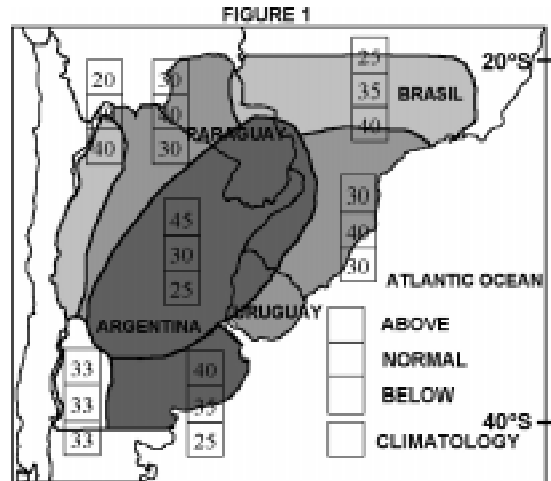


Figure 1 Geographical region of the COF of Southeast of South America and example of a seasonal precipitation forecast.

until early 2001, there was a strong El Niño at the beginning (1997-1998), followed immediately by a strong La Niña (1998-1999), that prolonged into 2000 as a cold event. This situation provided good grounds for the skill obtained. Some of the regions in which the COFs forecasts failed to provide useful results –most of the southern part, the western half and parts of southern Brazil- do not show a strong association with ENSO. Although ENSO is not the only source of forecast skill in the region, it certainly is an important one. The ENSO signature is probably present not only in the physical model forecasts, but also in the consensus discussions when interpreting the several diagnostic studies of seasonal climate variability conducted for the region.

We compare the skill score S of the COFs forecasts with that of the IRI seasonal precipitation predictions, the only source of physically based climate forecast that was always available at the COFs (Goddard et al., 2003), and available to us for the comparison. The details can be found in Berri et al. (2004), so here we provide only a summary. Figure 2b shows the averaged skill score S of 13 IRI seasonal precipitation forecasts and Figure 2c the averaged skill score S of the COFs forecasts for the same 13 periods (1998-2002). Overall, there is agreement in the areas with good performance -positive S - and with bad performance -negative S -. In general, the IRI forecast shows larger positive as well as negative S values in comparison with the COFs forecasts. This result indicates that the COFs forecasts, on average, assign a tercile probability distribution that is much closer to climatology than the IRI forecasts. Finally, the number of boxes with positive S values is 24 (or 38%) for the IRI forecasts and 19 (or 30%) for the COFs forecasts. In this sense, we can say that the performance of the IRI forecasts is slightly better than that of the COFs forecasts.

5. Discussion

Although the number of forecasts is small for a definitive conclusion about the quality of the COFs forecasts, they represent the result of five years of activities, which is a

considerable period of time in scientific research. The expected outcome of a consensus forecast should be the improvement of results over the individual pieces of information considered during the discussions. Unfortunately, we have only one source of forecast that was always available at the discussions and with the appropriate tercile presentation, i.e. the IRI forecasts, for comparison of results. In this sense, the results indicate that the consensus forecast not only adds no skill to the IRI forecast, but also provides an overall less skillful result. From a pessimistic point of view one could question the necessity of the COFs discussions since by simply adopting the IRI forecasts a better result, in the average, would have been achieved. However, the COF meetings are very important for the local community because they provide a forum for discussions among the climate researchers, and for the users an almost unique opportunity to have a direct contact with the climate researchers.

There is one important limitation to this evaluation that should be noted. Since predictability for many regions is seasonally dependent, skill may be higher, and thus useable, in certain seasons while not in others. Along the same lines, this period of 5 years, only has potentially 5 cases for a particular season. With such a small sample of forecasts, it is very difficult to draw strong conclusions about the skillfulness of forecasts for climate, which is inherently probabilistic. Future forecasts over regions for which the past forecasts were skillful are likely to be of value, although seasonality of skill is an important consideration. For regions where skill was weak or negative, longer series of forecasts are necessary to gain insight into whether or not the climate variability over these regions is actually predictable, and if so under what conditions and in what seasons.

The COFs over the last several years did suffer from a dearth of rigorous scientific methodology. It appears - following this study - that the process could benefit from more rigorous and documented methods to serve as the

foundation for the seasonal forecasts. A methodology should be established in order to assign, on an objective basis, the proper weights to the different pieces of information available during the discussions: forecasts from physical models, forecasts from statistical models and the result of climate diagnostic studies. The adoption of such a methodology will certainly facilitate the forum discussions and the preparation of the forecast. One final consideration to take into account is that the forecasters at the COFs often feel compelled to put something down on the map even if there isn't much reason for it. For example, the COFs always issued forecasts for the entire region regardless of the fact that in certain periods of the year and regions the models indicated an absence of skill. Perhaps it is the time to reconsider the seasons and the

regions where the seasonal precipitation forecasts will be issued.

References

- Berri, G.J., P. Antico and L. Goddard, 2004: Evaluation of the Climate Outlook Forums Seasonal Precipitation Forecasts of Southeast South America during 1998-2002, accepted *Int. J. Climatol.*
- Goddard L, A.G. Barnston and S.J. Mason, 2003, Evaluation of the IRI's 'Net Assessment' seasonal climate forecasts 1997-2001, *Bull. Amer. Meteor. Soc.*, 84, 12, 1761-1781.
- New, M., M. Hulme, and P. Jones, 1999: Representing twentieth-century space-time climate variability. Part I: Development of a 1961-90 mean monthly terrestrial climatology. *J. Climate*, 12, 829-856.

Are Intra-seasonal Oscillations 'Speed-breakers' to Seasonal Predictions?

R.H. Kripalani, Ashwini Kulkarni and S.S. Sabade
 Indian Institute of Tropical Meteorology, Pune 411 008, India
 Corresponding author: krip@tropmet.res.in

Introduction

The Indian summer monsoon rainfall variability is partly due to the external surface boundary forcing and partly due to its internal dynamics. Slowly varying surface boundary conditions such as the sea surface temperatures, snow cover etc. in the preceding winter and the pre-monsoon season are believed to constitute a major forcing on the inter-annual variability of the monsoon rainfall – these provide a handle for seasonal prediction by statistical and dynamical methods.

On several occasions the observed rainfall at the end of the season varies considerably from the forecasts issued. For example, none of the models could foreshadow the recent all-India droughts during Monsoon 2002 and 2004. This complexity may be due to the fact that the variability associated with the internal dynamics within the monsoon season is difficult to predict. The intra-seasonal variability dominant during the monsoon season constitutes this internal dynamics.

The hierarchy of quasi-periods dominant over the Indian region are the 3-7 days associated with the oscillation of the monsoon trough; the 10-20 days or quasi-biweekly oscillation associated with westward moving waves and the eastward moving 30-60 days mode or the 40-day mode now designated as Madden-Julian oscillations (MJOs). The northward movement of rainfall anomalies from the equatorial regions characterizes the 40-day mode over the Indian longitudes.

Attempts to examine the linkages between the intra-seasonal and inter-annual monsoon variability have been made (eg. Krishnamurthy and Shukla 2000; Sperber et al. 2000; Goswami and Ajaysmohan 2001; Lawrence and Webster 2001; Molteni et al. 2003; Waliser et al. 2003). Thus the problem is not new, neither is the solution

clearly established. Hence we re-examine here the relation between the intra-seasonal modes and the inter-annual monsoon variability with long daily rainfall observations for the 104-year period (1901-2004). The prime objective here is to show how these intra-seasonal modes could constitute a major hindrance (ie *Speed-breakers*) to seasonal predictability.

2. Data

The description of the data sets used in this article is as follows:

(i) Daily rainfall data for India as a whole for the period 1 June to 30 September 1901-1989 were prepared from grid data (Kripalani et al 1991) and for the period 1990-2004 updated from the *All India Weather Summary* prepared by the India Meteorological Department.

The daily mean climatology representing the seasonal cycle has been separately computed for the above two data sets. Daily precipitation anomalies are defined as departures from the daily mean climatology (separately for the above two periods). In effect this may be presumed to mean that this process has *removed the variability due to external surface boundary forcing*. This daily anomalous time series will contain fluctuations related with the intra-seasonal variability only.

(ii) The time series of seasonal (June through September) Indian monsoon rainfall (IMR) for the 104-year period has been downloaded from www.tropmet.res.in. The standardized IMR series is a measure of the intensity of the whole monsoon season.

3. Intensity of the Intra-seasonal Oscillations

To determine the intensity of these oscillations, the Butterworth band-pass filter (Murakami 1979) with peak response around the dominant periods is used. Thus half

power points at 3 and 7 days for the 3-7 days oscillations, at 10 and 20 days for the quasi-biweekly oscillations and at 30 and 60 days for the MJO are applied to the anomalous daily rainfall time series. The strength of the intra-seasonal oscillation is identified by first computing the variance of the unfiltered and filtered daily time series. The percentage of the original variance retained by the filtered time series is a measure of the intensity of these oscillations. These are computed for all the 104 years for all the 3 bands

To examine the relationship between the intensity of these oscillations and the seasonal monsoon rainfall and to identify the so-called 'Speed-breakers', scatter plots and correlation analysis between the percent variance in each band and the standardized IMR are determined.

4. Intra-seasonal Oscillations and Seasonal Monsoon Strength

4.1 3-7 days oscillations

Fig. 1 (page 17) shows the scatter plot between the standardized IMR and intensity of this mode. The scatter plot suggests a positive relationship, with correlation of +0.26 based on the 104-year period. A visual examination suggests that certain points appear as outliers and do not fit in the scatter plot. After eliminating these 20 points (shown as red dots in Fig.1) the correlation sharply increases to +0.60 based on 84 values, which is highly significant.

The eliminated years are distributed throughout the 104-year period. The minimum variance for these years is 7.4 % while the maximum is 30.1 %, indicating considerable variability of the mode. The standardized IMR varies from -1.6 to +2.0 ie it contains deficient, excess and normal monsoons. These years also contain 4 El Nino related years and 3 La Nina related years. In summary these years appear to be random and no clear reason can be assigned for their elimination – these are the *Speed-breakers* (red dots).

4.2 10-20 days oscillations

A similar scatter plot for this mode is shown in Fig.2. (page 17). The overall correlation is -0.05. However when certain years (red dots) are removed the correlation increases sharply to +0.67 based on 75 values, which is again highly significant. Again the eliminated years are distributed throughout the 104-year period. The intensity of this mode for the eliminated years varies from 4.7 to 34.0 %. The standardized IMR varies from -1.7 to +2.0 thus including full spectrum of monsoons from droughts to floods. These contain 6 (7) El Nino (La Nina) years. Again indicating that the eliminated years are random and can be designated as *Speed-breakers*.

4.3 30-60 days oscillations

The overall correlation of -0.15 sharply increases to -0.53 based on 86 values (Fig.3, page 17). Intensity varies from 4.0 to 31.5 % for the eliminated years; the standardized IMR varies from -2.4 to +1.3 and contains 5 El Nino and 2 La Nina years – suggesting randomness.

Among the deleted years (red dots in Fig. 1,2 and 3)) only 4 years (1905, 1920, 1934, 1951) are common again suggesting randomness. In spite of the deleted years evidence shows that the intra-seasonal modes can regulate the total summer monsoon precipitation regime in about 75 % of the years.

5. Summary and Discussion

In summary it can be inferred that the dominance of 3-7 and 10-20 days mode will favor monsoon activity over the Indian region, while the 30-60 days mode will not. This indicates a significant control by the intra-seasonal oscillations in determining seasonal monsoon strength. Such relationships have been shown earlier (eg. Kripalani et al 2004).

Thus the inverse (direct) relationship of the Indian monsoon with the slower (faster) modes should have some implication for seasonal prediction. However, it is difficult to estimate whether changes in intra-seasonal variability force changes in monsoon strength or vice versa. No clear relationship between the 30-60 days activity and global sea surface temperature has been found, suggesting that the 30-60 days variation may be internally or chaotically generated (Lawrence and Webster 2001). Attempts to predict these intra-seasonal oscillations are made (Sperber et al 2000 ; Waliser et al 2003), but still it is a challenge to forecast the behavior of these modes.

The fact that the eliminated years contain full spectrum of monsoons from droughts to floods, El Nino and La Nina years suggests that the intra-seasonal modes do not show difference in all the extreme monsoons nor show difference in all ENSO-related monsoons (Krishnamurthy and Shukla 2000 ; Sperber et al 2000). This suggests that the predictability is likely to be limited by chaotic internal variability of the monsoon system (Sperber et al 2000).

Lastly the *Speed-breakers*: Normally on the roads when one sees the speed-humps (*Speed-breakers*), some preventive action can be taken by slowing down. However, the Monsoon *Speed-breakers* are visualized after the monsoon is over, and by that time the value of the Seasonal Predictions has been severely reduced by these *Speed-breakers*.

References

- Goswami, B.N. and R.S. Ajayamohan 2001: Intra-seasonal oscillations and inter-annual variability of the Indian summer monsoon. *Journal of Climate*, 14, 1180-1198.
- Kripalani, R.H., A. Kulkarni, S.S. Sabade, J.V. Revadekar, S.K. Patwardhan and J.R. Kulkarni 2004: Intra-seasonal oscillations during Monsoon 2002 and 2003. *Current Science*, 87, 325-331.
- Kripalani, R.H., S.V. Singh and P.A. Arkin 1991: Large-scale features of rainfall and outgoing long-wave radiation over Indian and adjoining regions. *Contributions to Atmospheric Physics*, 64, 159-168.

- Krishnamurthy, V. and J. Shukla 2000: Intra-seasonal and inter-annual variability of rainfall over India. *Journal of Climate* 13, 4366-4377.
- Lawrence, D.M. and P.J. Webster 2001: Inter-annual variation of the intra-seasonal oscillation in the south Asian summer monsoon region. *Journal of Climate*, 14, 2910-2922.
- Molteni, F., C. Susanna, L. Ferranti and J.M. Slingo 2003: Predictability experiments for the Asian summer monsoon: Impact of SST anomalies on inter-annual and intra-seasonal variability. *Journal of Climate*, 16, 4001-4021.
- Murakami, M. 1979: Recursion technique for Band-pass filter. *Monthly Weather Review*, 107, 1011-1012.
- Sperber, K.R., J.M. Slingo and H. Annamalai 2000: Predictability and the relationship between sub-seasonal and inter-annual variability during the Asian summer monsoon. *Quarterly Journal of the Royal Meteorological Society*, 126, 2545-2574.
- Waliser, D.E., W. Stern, S. Schubert and K.M. Lau 2003: Dynamic predictability of intra-seasonal variability associated with the Asian summer monsoon. *Quarterly Journal of the Royal Meteorological Society*, 129, 2897-2928.

Mechanisms associated with the June–September 2003 Sahel Rainfall and Implications for Seasonal Climate Forecasts

Wassila M. Thiaw and Gerald D. Bell

Climate Prediction Center, National Centers for Environmental Predictions, NWS/NOAA

Corresponding author: Wassila.Thiaw@noaa.gov

1. Introduction

The Sahel is exceptionally sensitive to climate fluctuations on both interannual and interdecadal time scales. The prolonged droughts during the 1970s-80s have motivated many scientists to investigate the causes of such climate disasters and their impacts on water resources, food security, and health. However, a consensus on the mechanisms associated with Sahel rainfall variability has not yet been achieved. The influence of ENSO on the interannual variability of Sahel rainfall has been suggested (Ward, 1998, Janicot, 1996, Thiaw et al, 1999), while on the interdecadal time scale, the role of the inter-hemispheric difference in SST gradient has been addressed (Thiaw et al, 1999, Folland et al., 1986). Giannini et al. (2003) confirmed the role of equatorial Pacific SSTs on the interannual time scale, but suggested that warming of the oceans around Africa, in particular the warming trend in the Indian Ocean, may have favored a shift of convection from land to ocean resulting in the long term rainfall deficit in the Sahel. Chelliah and Bell (2004) recently indicated that these long-term rainfall fluctuations were associated with multi-decadal fluctuations in atmospheric convection and SSTs occurring throughout the global tropics, including the Indian Ocean, and therefore were not likely caused by anomalies in the Atlantic and/or African sectors alone.

In this paper we examine the atmospheric conditions associated with the above normal 2003 Sahel rainy season, which was the second wettest season since 1990 (not shown). We also assess the links to the leading tropical interannual (ENSO) and interdecadal modes of atmospheric and SST variability (Chelliah and Bell 2004). It is shown that improved Sahel rainfall predictions for a given season require accurate assessments of both the leading interannual and interdecadal modes, as well as accurate projections of their combined impacts on the West African monsoon system.

2. Spatial distribution of the 2003 Sahel rainfall

The Sahel, defined here as the region between 10°-20°N, 18°W-20°E (boxed region, Fig. 1), receives approximately 90% of its mean annual rainfall during June-September. The rainfall is monsoonal in character and is closely related to the north-south movement of the ITCZ, which starts its northward progression in March and reaches its northernmost position in August. Seasonal precipitation exhibits a strong meridional gradient, with average totals exceeding 600 mm in the south, and averaging 100-300 mm in the north. During 2003, above-normal rainfall occurred over much of the Sahel (Fig. 1a), with totals exceeding 100 mm above average across most of the central Sahel (Fig. 1b). The monthly rainfall departures increased as the season progressed (Fig 1c-f). Rainfall was above average nearly everywhere in June, except in the area 10-18W. By July positive rainfall anomalies extended further to the west, and in August/September anomalies over 50 mm were evident across the central and western Sahel.

3. Atmospheric circulation

3.1 Circulation during Aug-Sep 2003

Sahel rainfall is primarily controlled by the depth and northward penetration of the West African monsoon system, which in turn is related to the position of the mid- and upper-level jets. These larger-scale circulation features are fairly sensitive to changes in the global monsoon circulation on both the interannual and interdecadal time scales. The above-average 2003 rainy season was associated with an enhanced West African monsoon. At 925 hPa strong south-westerly winds averaging 6-9 m s⁻¹ extended well northward into the Sahel. This enhanced monsoonal inflow was also evident at 850 hPa (not shown) and contributed to a deep penetration of moist, unstable air well into the Sahel (Fig. 2). The enhanced monsoon was also associated with an anomalous low level cyclonic circulation across the northern and central Sahel, which contributed to the

development of active African waves that favored large convective rainfall totals throughout the region.

This anomalous cyclonic circulation reflected enhanced cyclonic shear along the equatorward flank of the African Easterly Jet (AEJ), and a northward shift of the mean AEJ to 17.5°N across the western Sahel (not shown). At upper levels the enhanced monsoonal circulation was associated with a strengthening of the subtropical ridges across both hemispheres (not shown), and with a corresponding amplification of the Tropical Easterly Jet. Consistent with the active rainfall season and the strengthening of the northern hemisphere subtropical ridge, above normal SSTs covered the northern Atlantic area near Africa in Aug-Sep 2003.

3.2 Multi-decadal signal

Sahel rainfall is marked by a sharp multi-decadal trend which can be linked to multi-decadal variations in the atmospheric circulation. Three indices based on the vertical wind shear, the 700-hPa easterly winds, and the relative vorticity along the equatorward flank of the AEJ, were constructed to diagnose the decadal trends in key areas of the West African monsoon system (Fig. 3). For the first half of the 1980s decreased wind shear (westerly shear anomalies) is evident over the Gulf of Guinea region (Fig. 3a). The easterly winds at 700 hPa are stronger than average (Fig. 3b), and anomalous anticyclonic relative vorticity is seen along the equatorward flank of the mean AEJ (Fig. 3c). This combination of conditions does not favor enhanced rainfall activity in the Sahel.

Since the mid-1990s we note a reversal in the sign of these trends. The circulation since that time has featured higher vertical wind shear (more baroclinic) over the Gulf of Guinea region, along with weaker easterly winds (westerly anomalies) at 700-hPa and anomalous cyclonic vorticity along the equatorward flank of the AEJ. This combination of conditions favors the development of rain producing African waves, as was observed during 2003. These conditions have also been associated with above-average SSTs across the northern Atlantic, and are consistent with the ongoing warm phase of the Atlantic multi-decadal mode (Landsea et al., 1999). The stronger monsoon circulations have also been associated with a significant increase in Atlantic hurricane activity since 1995, with the 1995-2003 period having the most tropical storms and hurricanes in any 9-yr period since the beginning of reliable records in 1944.

4. Discussion

The atmospheric conditions associated with the above-average 2003 Sahel rainy season are partly linked to the ongoing multi-decadal signal, which explicitly includes an above-average strength of the West African monsoon system. They are not associated with the ENSO-neutral conditions that prevailed throughout the season. Because of their link to the known multi-decadal fluctuations, the overall character of the atmospheric anomalies during

2003 could have been predicted prior to the season onset. This, in turn, would have led to predictions for above-average precipitation in the Sahel. However, since the exceptionally conducive nature of the atmospheric signal could not be accounted for by the multi-decadal signal alone, the amount of above-average rainfall that would have been predicted is limited.

Nonetheless, by July the enhanced monsoon circulation was already in place and the mean ITCZ was shifted well north of its mean position. At that time the AEJ, TEJ, and other key aspects of the monsoon system, indicated a continuation of an enhanced monsoon circulation through September. This information could have led to updated rainfall predictions for a high probability of a wet August-September period. This forecast approach, which relies heavily on the atmospheric components of the variability as opposed to just SST variability, is already in use by NOAA for making seasonal predictions of Atlantic hurricane activity. During 2003 these atmospheric conditions also provided guidance for accurate predictions of the above-normal 2003 Atlantic hurricane season.

Many seasonal rainfall prediction models for the Sahel use SSTs as the sole predictor. These forecasts did not predict the above-average 2003 rainy season because of a mixed set of SST anomalies. For example, SST anomalies in northern Atlantic were positive, but were counterbalanced by the warm sea surface in the Gulf of Guinea. Above-average SSTs in this region are associated statistically with below normal Sahel rainfall. To improve rainfall predictability in the Sahel, atmospheric anomalies in key areas must be taken into account and the multi-decadal signal must be better captured.

5. References

- Chelliah, M., and G. D. Bell, 2004: Tropical multidecadal and interannual climate variability in the NCEP-NCAR Reanalysis, *J. Climate*, 17, 1777-1803.
- Folland, C. K., T. N. Palmer, and D. E. Parker, 1986: Sahel rainfall and world-wide sea temperatures, 1901-85, *Nature*, 320, 602-607.
- Giannini, A., Saravanan, R., and P. Chang, 2003: Ocean forcing of Sahel rainfall on interannual to interdecadal timescales, *Science*, 302, 1027-1030
- Janicot, S., V. Moron, and B. Fontaine, 1996: Sahel droughts and ENSO dynamics, *Geophys. Res. Lett.*, 23, 515-518.
- Landsea, C. W., R. A. Pielke, A. M. Mestas-Nunez, and J. A. Knaff, 1999: Atlantic Basin hurricanes: Indices of climate changes. *Climate Change*, 42, 89-129.
- Thiaw, W., A.G. Barnston and V. Kumar, 1999: Predictions of African rainfall on the seasonal timescale, *J. Geophys. Res.*, 104, D24, 31589-31597.
- Ward, M. N., 1998: Diagnosis and short-lead time prediction of summer rainfall in tropical North Africa at interannual and multidecadal timescales, *J. Climate*, 12, 3167-3191.

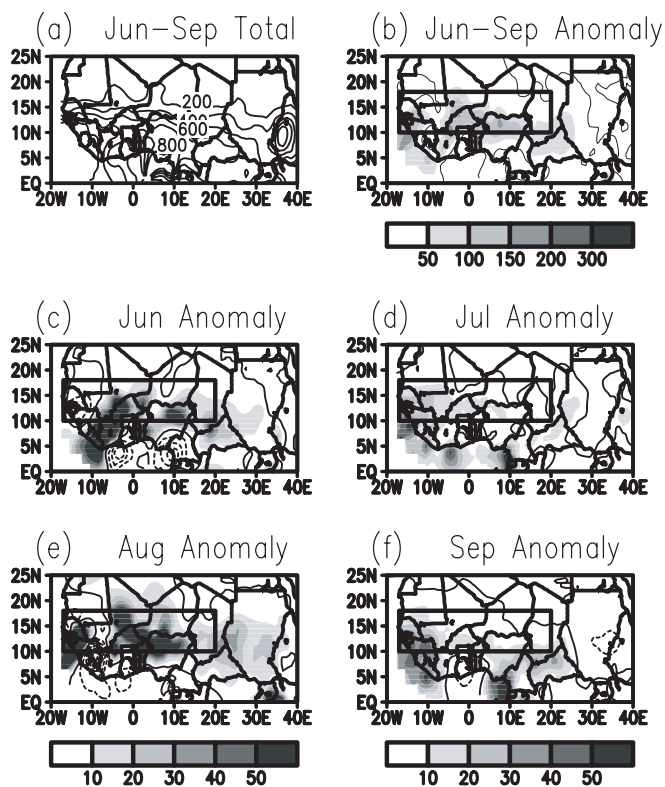


Fig. 1 (Top) Spatial distribution of West African rainfall during 2003: (a) mean (Jun-Sep) seasonal rainfall. (Middle and bottom) Monthly rainfall anomalies for June through September of 2003. Rainfall anomalies are with respect to the 1971-2000 climatology.

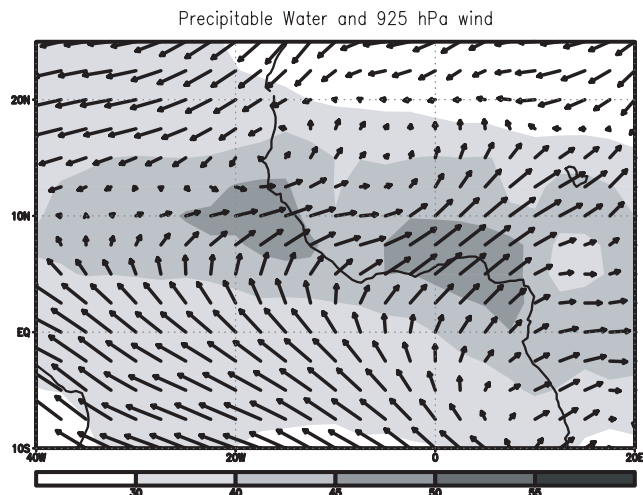


Fig. 2 Total precipitable water (mm) and 925 hPa vector winds over West Africa during Aug.-Sep. 2003.

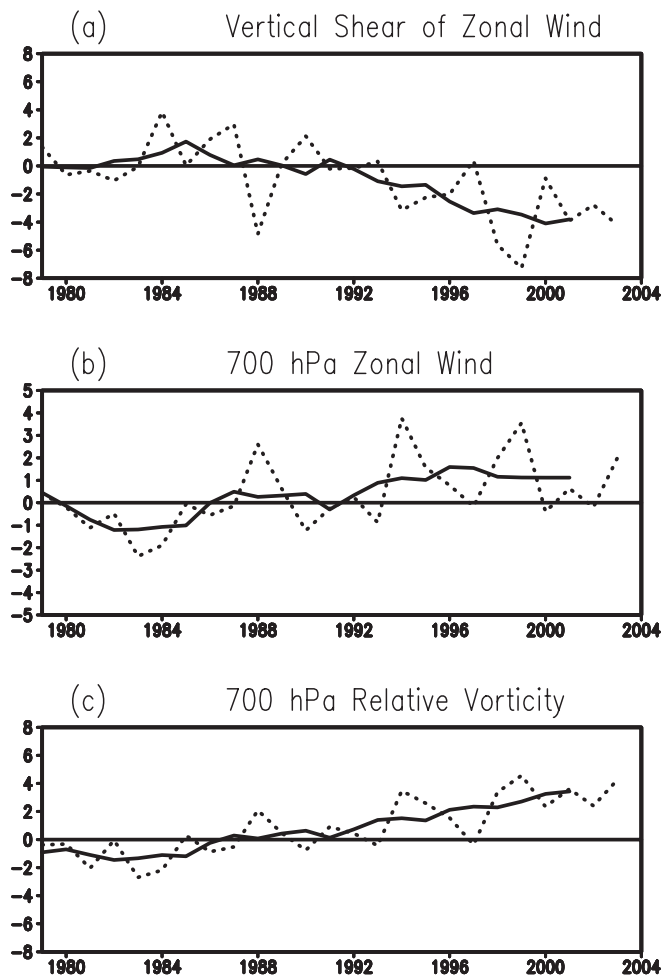


Fig. 3 Area-averaged anomaly time series for August-September period between 1979-2003: (a) 200-850-hPa vertical shear of zonal wind (ms^{-1}) for $17.5^{\circ}W-5^{\circ}E$; $5^{\circ}N-12.5^{\circ}N$, (b) 700-hPa zonal wind (ms^{-1}) for $20^{\circ}W-10^{\circ}E$; $5^{\circ}N-12.5^{\circ}N$, and (c) 700-hPa relative vorticity ($\times 10^6 s^{-1}$) for $17.5^{\circ}W-5^{\circ}E$; $7.5^{\circ}N-12.5^{\circ}N$. Black curves show un-smoothed two-month anomalies, and red curve shows a 5-pt running mean smoother applied to the time series shown. Anomalies are departures from the 1979-1995 base period monthly means.

Contents

Editorial	2
CLIVAR – The Regional/Global Dichotomy	2
The CLIVAR and Carbon Hydrographic Data Office at the UCSD Scripps Institution of Oceanography	3
Preliminary study of the East African short rains predictability at the monthly and grid–point scales (1968–1998)	5
Multi–Model Ensembling: Refining and Combining	8
The Predictability Barrier and Teleconnection Pattern Variability	11
From multi–model ensemble predictions to well–calibrated probability forecasts: Seasonal rainfall forecasts over South America 1959–2001	14
Seasonal Forecast of Antarctic Sea Ice	21
Seasonal climate prediction over South America using the CPTEC/COLA AGCM	23
Seasonal Precipitation Forecasts for the Southeast of South America. Evaluating the First Five Years	25
Are Intra–seasonal Oscillations ‘Speed–breakers’ to Seasonal Predictions?	27
Mechanisms associated with the June–September 2003 Sahel Rainfall and Implications for Seasonal Climate Forecasts	29
<p>Exchanges no. 31 – Apology to authors: Article page 21 “Seasonal to decadal predictability and prediction of southern African climate” shows incorrect affiliations for the authors. Affiliations should read: C.J.C. Reason – Oceanography, University of Cape Town M Tadross – EGS Department, University of Cape Town W. Landman, W. Tennant and M–J Kgatuke – South African Weather Service, Pretoria</p>	

The CLIVAR Newsletter Exchanges is published by the International CLIVAR Project Office
 ISSN No: 1026 - 0471

Editor: Howard Cattle
 Layout: Sandy Grapes

CLIVAR Exchanges is distributed free of charge upon request (icpo@soccc.soton.ac.uk)

Note on Copyright

Permission to use any scientific material (text as well as figures) published in CLIVAR Exchanges should be obtained from the authors. The reference should appear as follows: Authors, Year, Title. CLIVAR Exchanges, No. pp. (Unpublished manuscript).

If undelivered please return to:
 International CLIVAR Project Office
 Southampton Oceanography Centre, Empress Dock, Southampton, SO14 3ZH, United Kingdom